博士論文

令和 2 年度

Analyses of Ectodermal Transcription Factors and Identification of *Cis*-regulatory Elements for the Left-Sided *Nodal* Gene Expression during Embryogenesis of the Ascidian, *Halocynthia roretzi*

マボヤの胚発生における外胚葉転写因子および左側特異的 *Nodal* 遺伝子の発現制御領域の解析

大阪大学大学院理学研究科生物科学専攻

施 禹

INDEX

ABSTRACT

In developing embryos, appropriate gene expression mediates cell fate decision, differentiation, and morphogenesis. The spatiotemporal expression of zygotic genes is regulated by transcription factors. Investigation of the expression patterns and the transcriptional regulatory relationships is thus essential to understand embryonic development. The ascidian, *Halocynthia roretzi,* is a tunicate characterized by fast and invariant embryogenesis. Taking advantages of ascidian embryogenesis, gene regulatory networks for ectodermal development and left-right determination were analyzed.

First, spatiotemporal expression patterns and developmental roles of three transcription factors that are expressed in ectodermal cells of the early embryos were studied. Staged RNA-seq of the ascidian *H. roretzi* has previously suggested that these genes encoding transcription factors are transiently expressed at the blastula stage, which is the stage at which cell fates are specified and differentiation starts. In the present study, the expression patterns and functions of the transcription factors, FoxJ-r, SoxF, and SP8/9 were studied. The results showed that all three genes were expressed in the animal hemisphere as early as the 16-cell stage. Functional analyses using FoxJ-r morphants showed that they resulted in the disruption of laterality and the absence of epidermal mono-cilia, suggesting its functions in cilia formation and, consequently, in the generation of left-right asymmetry. SoxF knockdown resulted in incomplete epiboly by the ectoderm during gastrulation, while SP8/9 knockdown showed no phenotype until the tailbud stage in the present study, although it was expressed during blastula stages. These results indicate that transcription factor genes expressed at the cleavage stages play roles in diverse functions, and their roles are not limited to cell fate specification.

Second, the *cis*-regulatory elements of *nodal* gene were analyzed. The *nodal* signaling pathway plays an important role in establishment of the left-right axis during embryogenesis in many animals. Previous studies have shown that the left-sided expression of *nodal* gene in *H. roretzi* is triggered by the contact of left epidermis with and sensing vitelline membrane proteins. However, due to aggregation of the vitelline membrane proteins, it was difficult to identify the responsible proteins by biochemical methods. Here, using comparative genomics approach and reporter gene assay, I tried to identify the *cis*-regulatory elements of *nodal* gene. Phylogenetic footprinting analyses between two ascidian species suggested the putative regulatory regions locate both in the upstream region and the first intron. The reporter gene assay showed that -249 to -156 upstream region and the first intron both play crucial role for the left-sided *nodal* expression. In silico analysis provided a list of candidate receptor proteins that could be activated by the vitelline membrane signal for specification of the left-right asymmetry via the *nodal* expression.

The above results provide fundamental information for further studies on transcriptional regulatory relationships during embryogenesis, and shed a light on our understanding of embryonic development.

Chapter 1: Introduction

Embryogenesis, including cell divisions, cell fate specification, migration, differentiation, cell growth and death, is intricate biological processes that have been studied more than a century. To understand the early development, a number of the researches focused on the molecular mechanisms during key embryonic processes, such as gene expression, the spatiotemporal distribution of transcriptional factors, *cis*-regulatory elements of genes, and protein-protein interaction. However, studies of animal development, especially on vertebrates, have been often encountered difficulties caused by great amount of their cell number, complex embryonic structures, and slow developmental speed.

In this study, the ascidian *Halocynthia roretzi* was used as an experimental animal. As the closest relative to vertebrates in the phylogenetic tree, *Halocynthia* has been used as a model animal to study early embryonic development more than a century. It shows several advantageous characteristics, including small cell numbers, fast development, transparent embryos and invariant embryogenesis between individuals. Experimental techniques, such as microinjection and knockdown of gene functions, has been well established and matured. In addition, the cell linages were well described (Nishida and Stach, 2014) and the whole genome database is available (Dardaillon et al., 2020), making it a feasible model to access the gene regulatory network of *Halocynthia*. Some early developmental events, e.g. the maternal muscle determinant (Nishida, 2012) and the cell lineages and fate maps (Nishida and Stach, 2014) have been well described and analyzed in the previous studies. However, the full regulatory network of epidermis development (Imai et al., 2020) or the key determinants of left-right asymmetry establishment (Nishide et al., 2012; Tanaka et al., 2019; Yamada et al., 2019), are still elusive. Here, in order to further understand the embryogenesis of *Halocynthia*, two topics of embryonic development have been studied, (1) the function and expression patterns of three ectodermal transcription factors, FoxJ-r, SoxF and SP8/9, and (2) the *cis*-regulatory elements for the left-sided expression of *nodal* gene.

(1) Expression and functional analyses of ectodermal transcription factors, FoxJ-r, SoxF, and SP8/9, in early embryos. The spatiotemporal expression of zygotic genes is regulated by transcription factors (Satou et al., 2001; Kumano et al., 2014). Staged RNA-seq of the ascidian *Halocynthia roretzi* in six developmental processes has previously shown that nine genes encoding transcription factors are transiently expressed at the blastula stage, which is the stage at which cell fates are specified and differentiation starts. Six of these transcription factors have already been found to play important roles during early development. However, the functions of the other transcription factors (FoxJ-r, SoxF, and SP8/9) remain unknown. The study of the spatial and temporal expression patterns showed that all three genes were expressed in the animal hemisphere as early as the 16-cell stage. The functions of these genes were analyzed using antisense Morpholino oligos. The study is described in Chapter 2.

(2) Analyses of *cis*-regulatory elements of *nodal* gene for the left- sided expression. The *nodal* signaling pathway plays important roles in establishment of the left-right axis during embryogenesis in many animals (Levin et al., 1995; Morokuma et al., 2002; Montague et al., 2018). In *Halocynthia*, neurula embryos rotate along the anterior-posterior axis, and then cease the rotation when the left-side comes down, making the left-sided epidermis cells contacting with the vitelline membrane (Nishide et al., 2012). The left-sided expression of *nodal* gene is triggered by the contact of left epidermis with and sensing vitelline membrane proteins. Chemical signals from the vitelline membrane, which has been shown to be protein components, induce the left-sided *nodal* gene expression and eventually promote the morphological left-right asymmetry (Tanaka et al., 2019). However, due to aggregation of insoluble vitelline membrane proteins, it was difficult to identify the responsible proteins by biochemical methods. It has been also unknown how the vitelline membrane proteins drive *nodal* gene expression in the epidermal cells. I approached the issue from the reverse direction by investigating *cis*-regulatory elements of *nodal* gene that respond to the vitelline membrane proteins. Here, by using comparative genomics approach and reporter gene assay, the *cis*-regulatory elements of *nodal* gene were analyzed. The study is described in the Chapter 3.

These results advanced our understanding of the transcriptional regulatory network in ascidians.

Chapter 2
Expression and Functional Analyses of Ectodermal Transcription Factors

2-1. Introduction

Maternal products and zygotic gene expression control early developmental processes. The spatiotemporal control of zygotic expression, which is mediated by transcription factors, results in cell fate decision and differentiation. Identifying these transcription factors and understanding the transcriptional regulatory relationships are ways to improve our understanding of embryogenesis.

In ascidians, the zygotic expression of various transcription factors is initiated during cleavage to blastula stages. The corresponding spatiotemporal expression patterns and their developmental functions have been investigated extensively (Imai et al., 2004; Nishida, 2005; Imai et al., 2006). To identify additional potential key regulators in the embryogenesis of ascidians, transcriptome analysis by RNA-seq of *Halocynthia roretzi* embryos was carried out at six developmental stages from fertilized eggs to tadpole larvae [Wang K., Lemaire P., Nishida H., unpublished data. The data were deposited in the Aniseed database (https://www.aniseed.cnrs.fr/; (Dardaillon et al., 2020) and are publicly available (Select transcript model of a gene of interest on the genome browser. Show its gene card. The temporal expression profile is shown graphically in "Expression" tab.)]. Based on the profiling of temporal expression patterns using RNA-seq data, nine zygotic genes of transcription factors (*Tbx6, SoxB1, ZicN, FoxDa, Notlc, Lhx3, SP8/9, FoxJ-r,* and *SoxF*) showed peaks in the expression level at the blastula (110-cell) stage when cell fate specification was ongoing (Fig. 1). These genes have no maternal transcripts, and their zygotic expression peaks at the blastula stage. This indicates that they may play roles in early embryogenesis. Six of these transcription factors have already been analyzed in previous studies, and have been found to play crucial roles in cell fate specification, such as Tbx6 in mesenchyme and muscle fate determination (Kumano et al., 2014) and Lhx3 in endoderm formation (Satou et al., 2001). The other three transcription factors (FoxJ-r, SoxF, and SP8/9) could play roles in *Halocynthia* embryogenesis. In the present study, I investigated the spatiotemporal expression patterns and functions of these three genes in detail.

FoxJ-r is a member of the forkhead family transcription factor, containing a forkhead (winged helix) domain for DNA-binding. FoxJ plays a critical role in regulating the expression of genes that are required for the formation of motile cilia in vertebrates, including the cilia in the human airway, Kupffer's vesicle in zebrafish, nodes in mice, and the gastrocoel roof plate of *Xenopus* (Yu et al., 2008; Didon et al., 2013; Li et al., 2018). In some mammals, the generation of the left-right (L-R) asymmetry of the body involves motile cilia function, and FoxJ has also been found to contribute to the L-R asymmetry in zebrafish and mice (Tian et al., 2009). In

ascidians, epidermal motile cilia also contribute to the formation of L-R asymmetry by driving neurula rotation (Yamada et al., 2019).

SoxF is a member of the SRY-related HMG-box (SOX) family and contains a high-mobility group (HMG) domain, which is expected to be a DNA-binding domain. In humans, it is involved in the determination of the cell fate regulation of hemogenic endothelium (Sim and Chow, 1999). SoxF has been shown to play a pivotal role in cardiovascular development and early endoderm formation in zebrafish (Chan et al., 2009; Francois et al., 2010). SoxF also drives early endoderm gene expression in *Xenopus* (Ahmed et al., 2004) and mediates the negative-feedback loop of the *Drosophila* wingless pathway (Dichtel-Danjoy et al., 2009) and the VEGF activity of angiogenesis in mice (Kim et al., 2016).

The SP8/9 transcription factor belongs to the SP family. It contains the Btd box and SP box found in other SP family genes (Bouwman and Philipsen, 2002), as well as two zinc finger motifs, Cys-2–His-2, for target gene binding. In mice, SP8 and SP9 are essential and are necessary for limb development (Haro et al., 2014). SP8 and 9 are also expressed during fin or limb outgrowth in other vertebrates (Bell et al., 2003; Treichel et al., 2003; Kawakami et al., 2004).

In this study, I characterized the spatiotemporal expression pattern using in situ hybridization, and analyzed the morphant phenotypes of three transcription factors, namely FoxJ-r, SoxF, and SP8/9, none of which have been previously studied in *Halocynthia*.

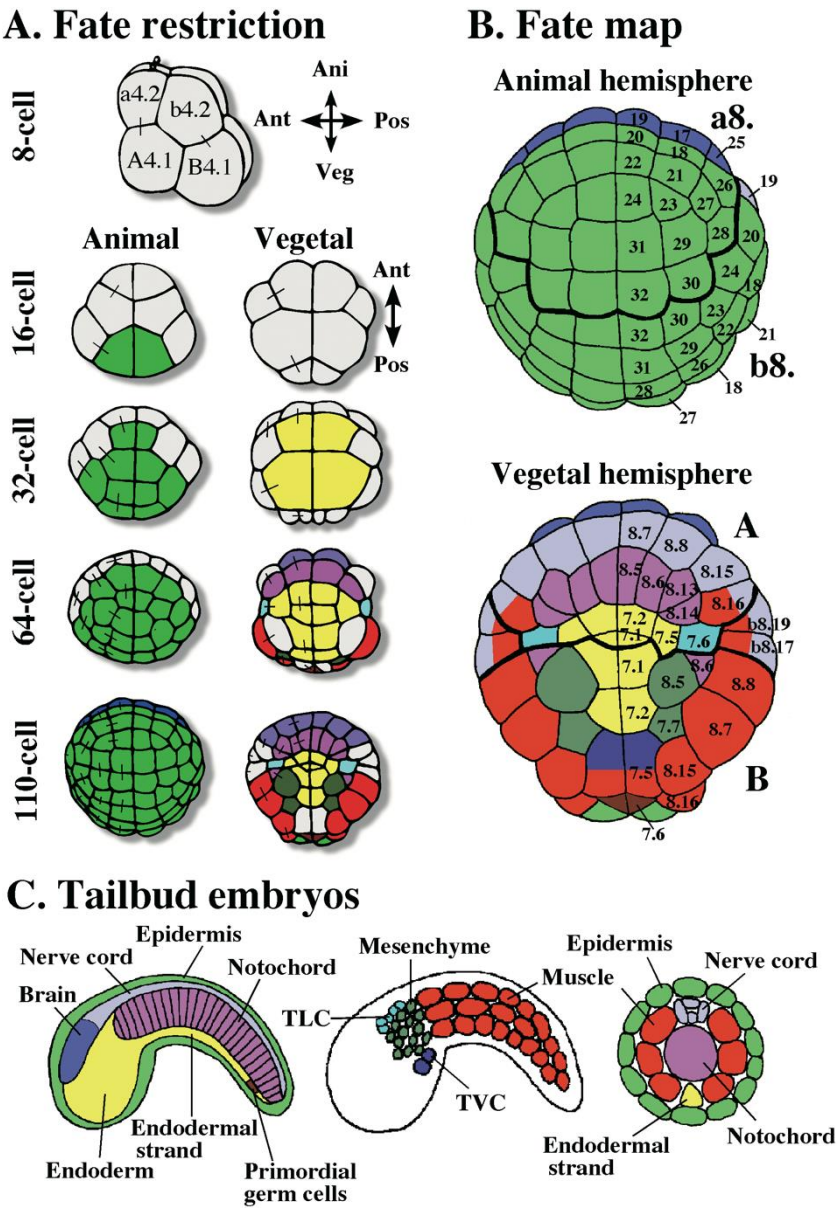

Fig. 1. Developmental fates of blastomeres of the ascidian embryo (Reproduced from Nishida, 2005)

(A) Fate restriction during cleavage stages in the animal (left) and vegetal (right) hemispheres. Blastomeres are colored when the fate of the blastomere is restricted to give rise to a single kind of tissue cell type. The colors of blastomeres correspond to the colors of larval tissues indicated in (C). Sister blastomeres of the previous cleavage are connected by bars. (B) Fate map of the 110-cell stage. Animal and vegetal hemispheres. Names of blastomeres are indicated as 'a8.19' etc. (C) Organization of tailbud embryos. Mid-sagittal planes, sagittal planes, and transverse sections of the tail (from left to right drawings, respectively). (Nishida, 2005)

2-2. Results and Discussion

In the present study, I investigated the spatiotemporal expression patterns of three transcription factor genes, namely *FoxJ-r*, *SoxF*, and *SP8/9*, using in situ hybridization. Their functions in early embryos were investigated by translation inhibition using MOs.

2-2-1. FoxJ-r

The FoxJ-r transcription factor of *Halocynthia* contains a forkhead domain (amino acids 266–350) and appears to be a member of the FoxJ family in the phylogenetic tree (see Supplementary Figure S1, red rectangle). By searching for FoxJ in the *Halocynthia* genome, I found that there is another transcription factor (FoxJ1) that is more similar to FoxJ1 in vertebrates. Consistently, there are two FoxJ homologs in the genome of another ascidian, *Ciona* (see Supplementary Figure S1, blue underlines). Therefore, I named the gene *FoxJ-related* (*FoxJ-r*). Although some bootstrap values were low in the phylogenic tree, FoxJ-r is highly likely a member of the FoxJ family since the blasting of the entire sequence of *Halocynthia* FoxJ-r in NCBI resulted in FoxJ hits in various animals.

The temporal expression pattern obtained from the reads per kilobase of exon per million mapped sequence reads (RPKM) data indicates that *FoxJ1* is not expressed in the embryonic development of *Halocynthia*, although the FoxJ1 protein sequence is more similar to vertebrate FoxJ. In contrast, *FoxJ-r* was preferentially expressed at the blastula stage (Fig. 2A). In situ hybridization showed that a small amount of maternal *FoxJ-r* mRNA in *Halocynthia* was present and localized to the centrosome-attracting body (CAB) (Makabe and Nishida, 2012) at the 16-cell stage (Fig. 2B, arrowheads). Similar maternal localization to the CAB was also observed for the *Foxj2* mRNA of *Ciona* in its database (http://ghost.zool.kyoto-u.ac.jp/cgi-bin/gb2/gbrowse/kh/). Then, *FoxJ-r* was transiently detected in the nuclei of all animal hemisphere cells at the 16- and 32-cell stages. From the 64-cell stage, the expression was turned on in the vegetal side, A7.3, A7.4 (notochord precursors), A7.7, A7.8 (nerve cord precursors), A7.6 (trunk lateral cell precursor), and B7.3 (mesenchyme precursor) cells. From the 110-cell stage to the gastrula stage, the expression diminished in most cells, but persisted in the nerve cord precursors. During the neurula stage, *FoxJ-r* was expressed in the neural fold, most likely by cells of nerve cord precursors that developed into ependymal glia cells, which are responsible for extending cilia towards the neural tube cavity (Crowther and Whittaker, 1992; Konno et al., 2010). In addition, a novel expression pattern was observed in the anterior bilateral region (Fig. 1B, arrow). At the tailbud stage, the brain area showed *FoxJ-r* expression (Fig. 2C), in addition to sparse expression in the nerve cord.

FoxJ plays a critical role in activating the gene expression required for the formation of motile cilia in vertebrates (Yu et al., 2008; Didon et al., 2013). Since the left-right asymmetry is established by motile cilia in zebrafish, FoxJ has also been found to contribute to the formation

of L-R asymmetry (Tian et al., 2009). Therefore, I checked the laterality of *Halocynthia* embryos and larvae in FoxJ-r knockdown embryos. A normal *Halocynthia* neurula rotates along the anterior-posterior axis until the left side faces downward by neurula rotation, driven by epidermal mono-cilia. Then, direct contact between the left side of the neurula and the vitelline membrane triggers *nodal* gene expression in the left-side epidermis. Morphological L-R asymmetries become evident in the tadpole larvae: the brain vesicle and sensory pigment cells are located on the right side of the trunk, and the tail bends towards the left within the limited perivitelline space (Nishide et al., 2012; Tanaka et al., 2019). When FoxJ-r MO was injected into eggs, the resulting embryos showed abnormalities in laterality, although they could eventually develop into tadpole-shaped larvae. In neurulae with FoxJ-r knockdown, approximately half of the morphants did not rotate during the neurula stage. Random positioning was observed in the sensory pigment cells and the orientation of tail bending at the pre-hatching larval stage was also randomized (Fig. 3A). Similar abnormalities have been previously observed in embryos in which nodal signaling is inhibited (Nishide et al., 2012). Therefore, I investigated *nodal* gene expression in the neurula and initial tailbud embryos. In the controls, *nodal* was expressed on the left in most embryos (n = 5, 80%). In contrast, *nodal* was expressed on the left side (n = 43, 35%), on the right side (12%), on both sides (30%), or simply not expressed (23%) in knockdown embryos (Fig. 3A, B). Therefore, *nodal* gene expression on the L-R axis was disrupted in morphant embryos. In addition to approximately half of the morphants failing neurula rotation, I also observed epidermis monocilia using scanning electron microscopy. Many epidermal cells were found to lack monocilia at the neurula stage (n = 34, 71%), while the control embryos injected with the control MO appeared normal (n = 5, 100%; Fig. 3C). The zygotic expression of *FoxJ-r* at the 32- and 64-cell stages was observed in every animal hemisphere cell that gave rise to the epidermis. The morphant phenotype suggests that FoxJ-r functions in promoting the expression of genes that are required for the formation of epidermal cilia, as observed in vertebrates.

The expression of *FoxJ-r* starting from the 110-cell stage to the tailbud stage in the progenitor cells of nerve cord ependymal glia, which form cilia into the neural tube cavity, suggests its possible function in ciliogenesis, as previously suggested in mice (Li et al., 2018). In zebrafish, *foxj1a* and *foxj1.2* are expressed in the Kupffer's vesicle and other organs with cilia (Aamar and Dawid, 2008). *foxj1a* is essential for the activation of genes encoding components of motile cilia, such as *dnah9* and *cetn2*, and the ectopic expression of foxj1a induces motile cilia-like cilia in non-ciliated cells (Yu et al., 2008). This approach would also be feasible for further functional analysis of FoxJ-r in *Halocynthia* in future studies. The functions of its broad expression in the brain at the tailbud stage in *Halocynthia* are elusive. In mice, FoxJ1 is transiently expressed in several neural subtypes during development and is required for cell fate determination (Li et al., 2018). However, in *Halocynthia*, FoxJ-r morphants did not show any

evident morphological abnormalities in the hatched larvae, except for laterality. Thus, further analysis will be needed to fully elucidate the role of FoxJ-r in the brain.

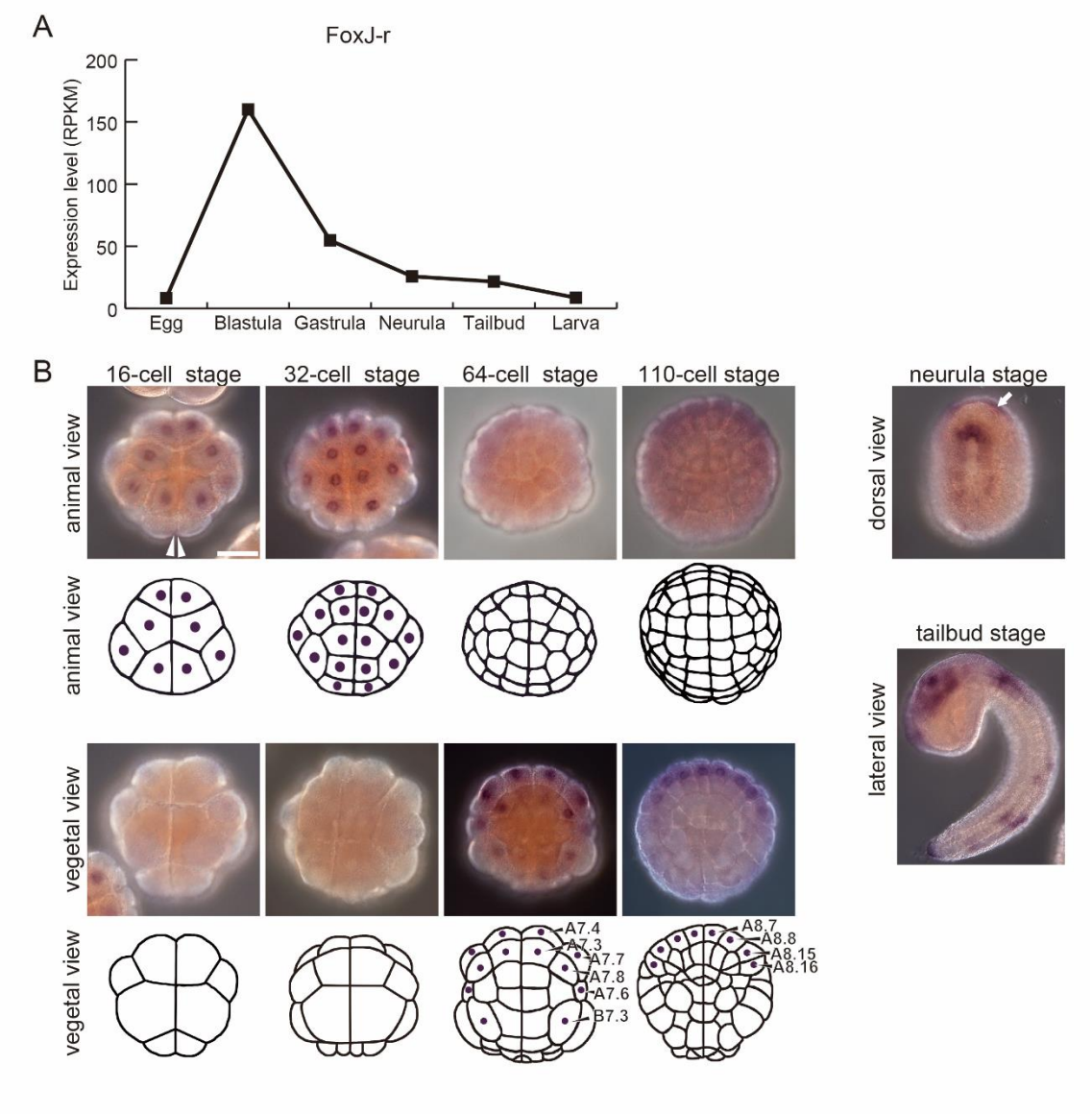

Fig. 2. Expression pattern of *FoxJ-r*. **(A)** Expression level is shown as the RPKM (reads per kilobase of exon per million mapped sequence reads) value of *Fox-r* using RNA-seq data. **(B)** In situ hybridization of *FoxJ-r* from the 16-cell stage to tailbud stage. Orientations of embryos are indicated on the left of each panel. Anterior is up. Purple dots in the cartoon indicate nuclear staining. Note that maternal transcripts are present in the CAB (arrowhead). Arrow denotes the anterior expression at the neurula stage. Scale bar, 50 μm.

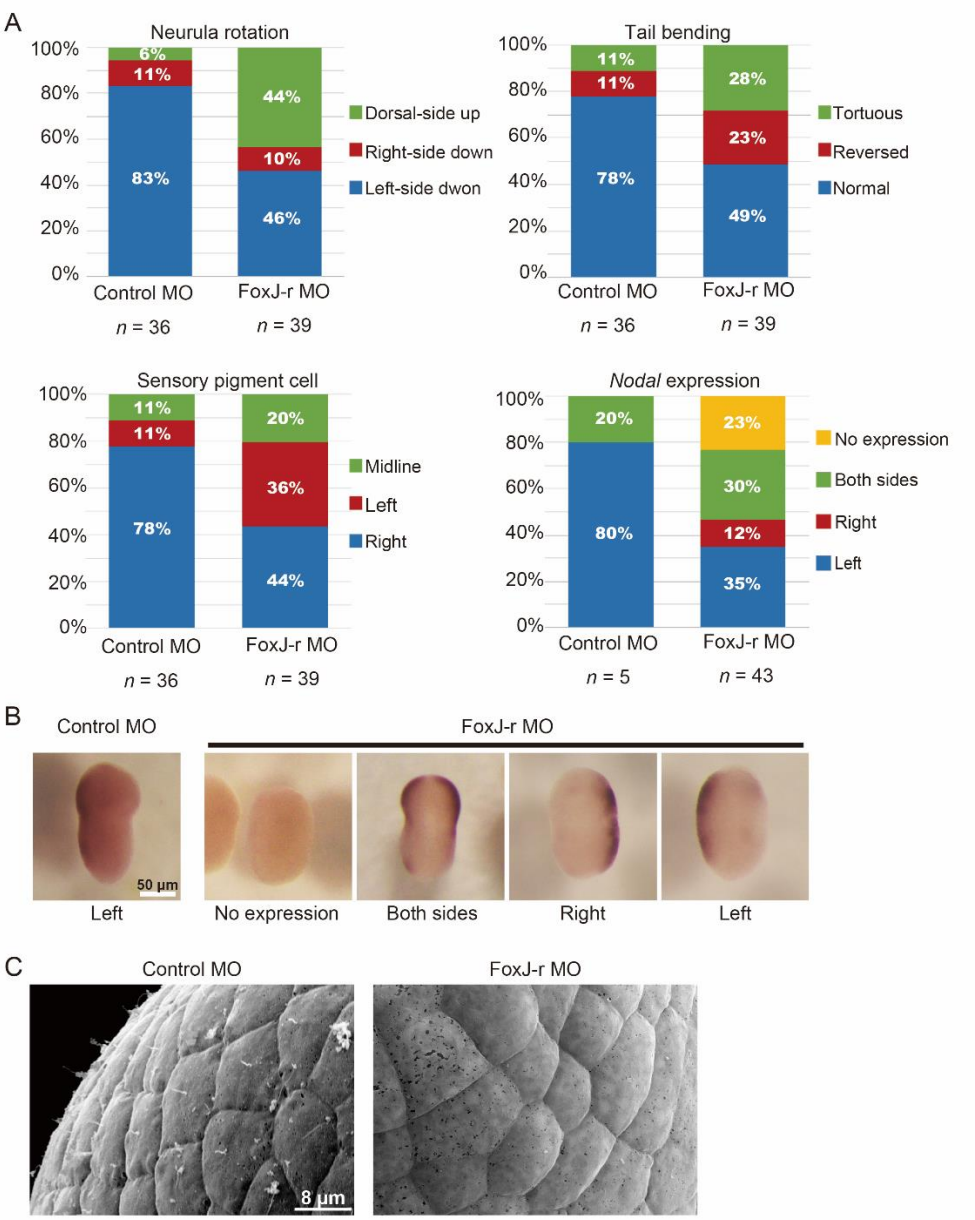

Fig. 3. Disruption of laterality by FoxJ-r MO. **(A)** Phenotypes of embryos injected with a FoxJ-r MO at the neurula and larval stages. Left to right: Occurrence of the neurula rotation, direction of the tail bending, position of the sensory pigment cells, and *nodal* gene expression. The rotation of embryos was evaluated at the neurula stage when the normal embryos stayed on the left side after the neurula rotation at 15 h after fertilization. The direction of tail bending and position of sensory pigment cells were monitored at the larval stage prior to hatching at 35 h of development. **(B)** *Nodal* expression visualized by in situ hybridization at the late neurula and initial tailbud stages (~18 h). Anterior is up. **(C)** Embryos injected with a FoxJ-r MO were observed by scanning electron microscopy at the neurula stage to visualize the epidermal cilia.

2-2-2. SoxF

The HMG box domain (amino acids 118–186) and phylogenetic tree indicated that this transcription factor was SoxF (see Supplementary Figure S2). The SoxF family consists of Sox18, 17, and 7. *Halocynthia* and *Ciona* SoxF are located at the base of the vertebrate Sox18, 17, and 7. Although the bootstrap value supporting this was low in the phylogenic tree, the blasting of the entire sequence of *Halocynthia* SoxF resulted in a large number of hits, mostly in the SoxF family in various animals. The RNA-seq data indicated that *SoxF* was expressed from the 16-cell stage to larvae, with its peak at the blastula stage (Fig. 4A). The in situ hybridization of *SoxF* showed that it was transiently expressed in all animal hemisphere cells from the 16-cell to 32-cell stage. At the 64-cell stage, only the cytoplasmic signal was detected in the animal hemisphere, and *SoxF* turned on in the cells of A7.6, B7.1, and B7.2 in the vegetal side. Its expression was not detected at the 110-cell stage, whereas expression began again at the gastrula stage. Strong expression was detected at the neurula stage in mesenchyme precursor cells. At the tailbud stage, *SoxF* was found to be expressed in the mesenchyme (Fig. 4B).

SoxF MO was injected to observe the morphant phenotype. SoxF-knockdown embryos showed two abnormal phenotypes: the first showed halted development during gastrulation and development into a disorganized cell mass (n = 148, 40%) (Class 1, Fig. 5A, left), while the other showed ceased development at the initial tailbud stage (n = 148, 58%) (Class 2, Fig. 5A, right). Some cells protruded outside the embryos and larvae from the section not covered by the epidermis. The detection of tissue differentiation markers, Mu-2, Not-1, and Epi-2 antigens, showed that, even in the cells of the disorganized mass (Class 1), a reduced amount of differentiated muscle, notochord, and epidermis were present (Fig. 5B-D; muscle, n = 16, 40%; notochord, n = 34, 26%; epidermis, n = 8, 63%). The class 2 embryos also showed muscle and notochord markers (muscle, n = 21, 52%; notochord, n = 23, 57%; epidermis, n = 6, 83%). Most parts of the smooth surface of Class 1 and 2 embryos were covered by Epi-2-expressing epidermis cells. On the other hand, the protruding cells never expressed the epidermal marker, suggesting that the closure of the blastopore was not completed (Fig. 4D). Thus, it is possible that cell differentiation, including epidermis formation, proceeded to some extent, but that the epiboly of the ectoderm was affected, resulting in the failure of blastopore closure in the SoxF morphants. However, it remains difficult to infer the detailed functions of this gene, since the phenotype was variable and only the failure of blastopore closure could be confirmed.

A SoxF family member, Sox17, is known to be involved in the early steps of endoderm cell fate specification in *Xenopus*, zebrafish, and mice (Tam et al., 2003). In contrast, SoxF is exclusively expressed in the animal hemisphere at early developmental stages in *Halocynthia*. The transcription factors Titf (NK-2 family, the same as Ttf) and Lhx3 are specifically expressed in endoderm precursors at the blastula and gastrula stages, and have been reported to play roles in endoderm cell fate specification in ascidians (Ristoratore et al., 1999; Spagnuolo and Di

Lauro, 2002). These findings suggest that the gene regulatory cascade of endoderm formation diverges between ascidians and vertebrates.

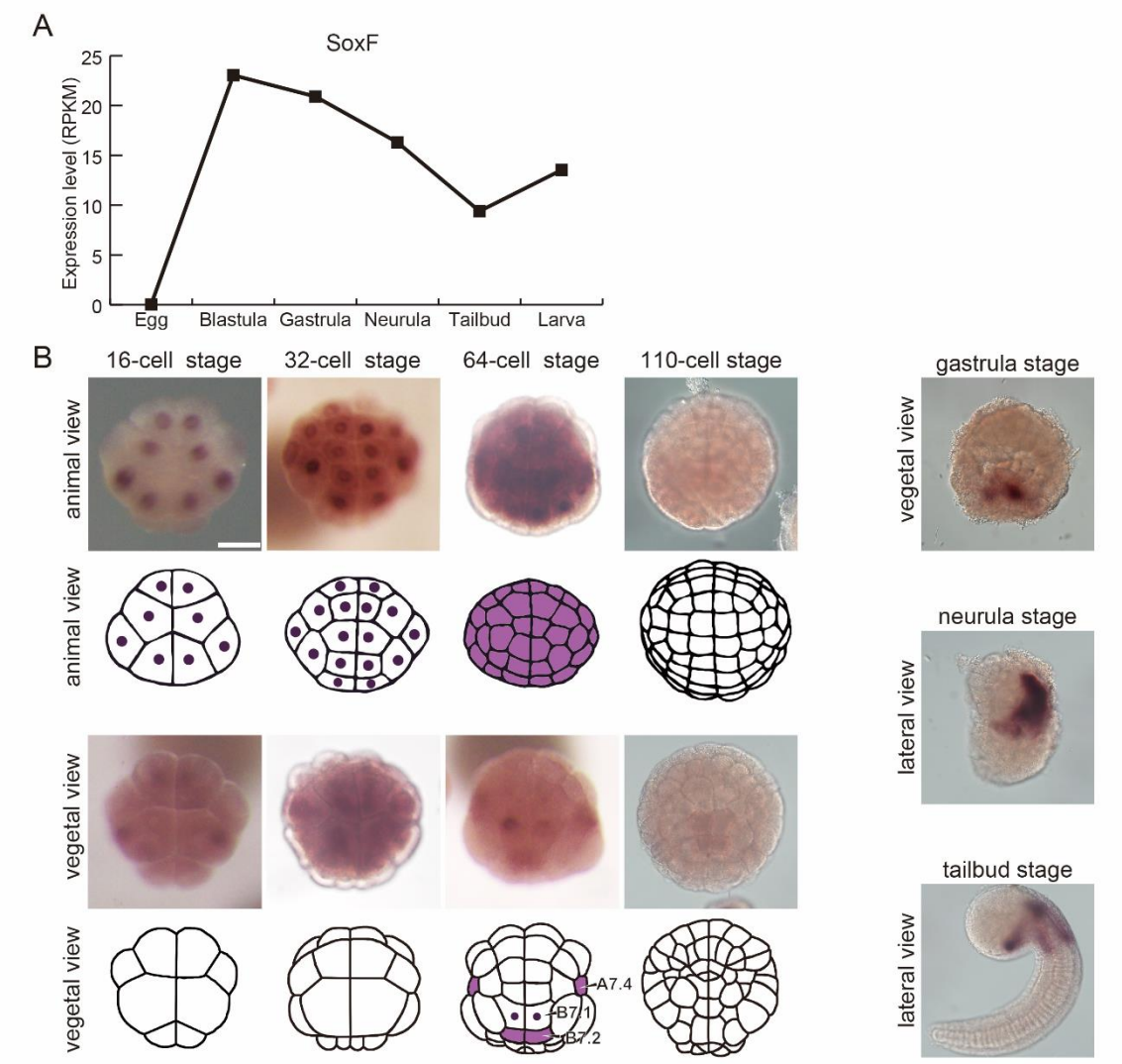

Fig. 4. Expression pattern of *SoxF*. **(A)** RPKM value of *SoxF* counted from RNA-seq data. **(B)** In situ hybridization for *SoxF* from the 16-cell to tailbud stages. Anterior is up. Signal in the vegetal views at the 16- and 32-cell stages is actually that of the animal hemisphere. Purple dots in the cartoon indicate nuclear staining. Purple painting of cells shows cytoplasmic staining. Scale bar, 50 μm.

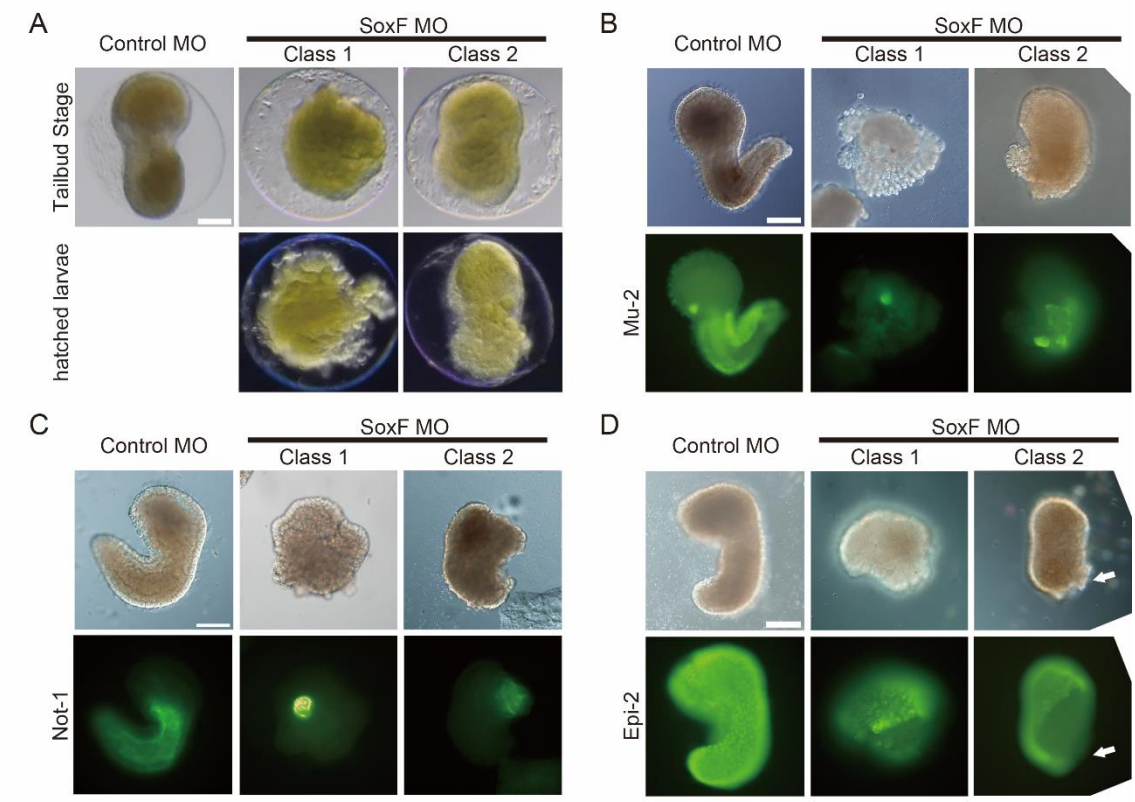

Fig. 5. SoxF MO-injected embryos and tissue differentiation. **(A)** Morphology of embryos at the middle tailbud stage and hatched larval stage, although morphants did not hatch. Left to right: Control MO, embryo injected with SoxF MO that showed a severe phenotype (Class 1), and embryo injected with SoxF MO that showed a milder phenotype (Class 2). **(B)** Muscle differentiation detected with Mu-2 antibody at the tailbud stage. Bottom row shows the Mu-2 antibody staining. Morphants had muscle cells in both Class 1 and 2 embryos. **(C)** Notochord differentiation detected with Not-1 antibody at the tailbud stage. **(D)** Epidermis differentiation detected with Epi-2 antibody at the tailbud stage. Most of the smooth surface of the embryos in Class 1 and 2 embryos was covered by Epi-2-expressing epidermis cells, while the protruding cells (arrows) never expressed the epidermis marker. Scale bar, 50 μm.

2-2-3. SP8/9

SP8/9 of *Halocynthia* contains an Sp domain (amino acids 5–20), a Btd box (amino acids 306–317, and two zinc finger motifs Cys-2-His-2 (amino acids 317–415). Based on the phylogenetic tree, this transcription factor is likely to be an SP8/9 homolog (see Supplementary Figure S3). Ascidian homologs are found at the base of vertebrate SP8 and 9. The temporal expression pattern obtained from the RNA-seq data suggests that *SP8/9* expression peaks sharply at the blastula stage (Fig. 6A), which is consistent with the in situ hybridization results. Nuclear signals were detected in all animal cells at the 16- to 32-cell stage. The cytoplasmic signal persisted after the 64-cell stage. From the gastrula stage, the signal disappeared, and strong expression was observed in the anterior terminal of the tailbud embryos (Fig. 6B).

Despite injecting MO of SP8/9, all morphant larvae showed mostly normal morphologies, except for a slightly kinked tail (normal, n = 17, 94%; Fig. 7A), with a trunk and tail covered entirely by morphologically normal epidermis. As SP8/9 was expressed in the entire animal hemisphere during the cleavage stages, I examined epidermal differentiation. The epidermis marker, Epi-2 antigen, was found to be normally expressed at the tailbud stage, as in controls (n = 10/10, 100%; Fig. 7B). Thus, the epidermis looked morphologically normal and expressed the epidermal differentiation marker. These results indicate that SP8/9, which is expressed at the cleavage stages, may not play any particular role in the formation and morphogenesis of epidermis up to the tailbud stage in *Halocynthia* early embryos. Nevertheless, it was exclusively expressed in animal hemisphere blastomeres. Alternatively, the present MO may not be efficient in suppressing SP8/9 translation. However, the same result was observed in *Ciona*, where the morphants of *Zf220* (SP8/9 of *Ciona intestinalis*) showed normal morphology until the middle tailbud stage, but resulted in the perturbation of gene expression in the palp-forming area (the anterior terminal of the tailbud embryos) (Liu and Satou, 2019). Other possibilities include that loss of SP8/9 is compensated by other genes, or that its target genes are redundantly regulated by other transcription factors. For example, in mice, the apical ectodermal ridge (AER) patterning in the limb bud is regulated by both Sp8 and Sp6. Therefore, losing one of these does not result in an abnormal phenotype (Haro et al., 2014). The identification of potential transcriptional target genes of SP8/9 may be necessary to improve our understanding of the regulatory relationships of the downstream genes.

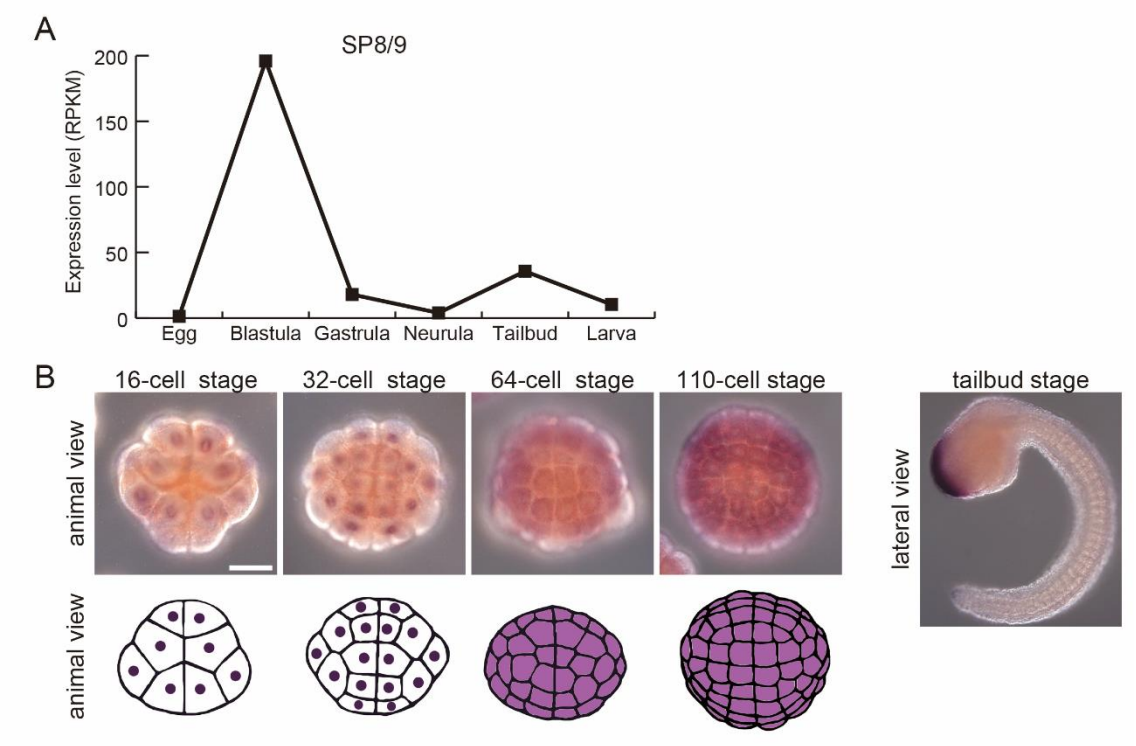

Fig. 6. Expression pattern of *SP8/9*. **(A)** The RPKM value of *SP8/9* counted from RNA-seq data. **(B)** In situ hybridization for *SP8/9* from the 16-cell stage to tailbud stage. Anterior is up. Scale bar, 50 μm.

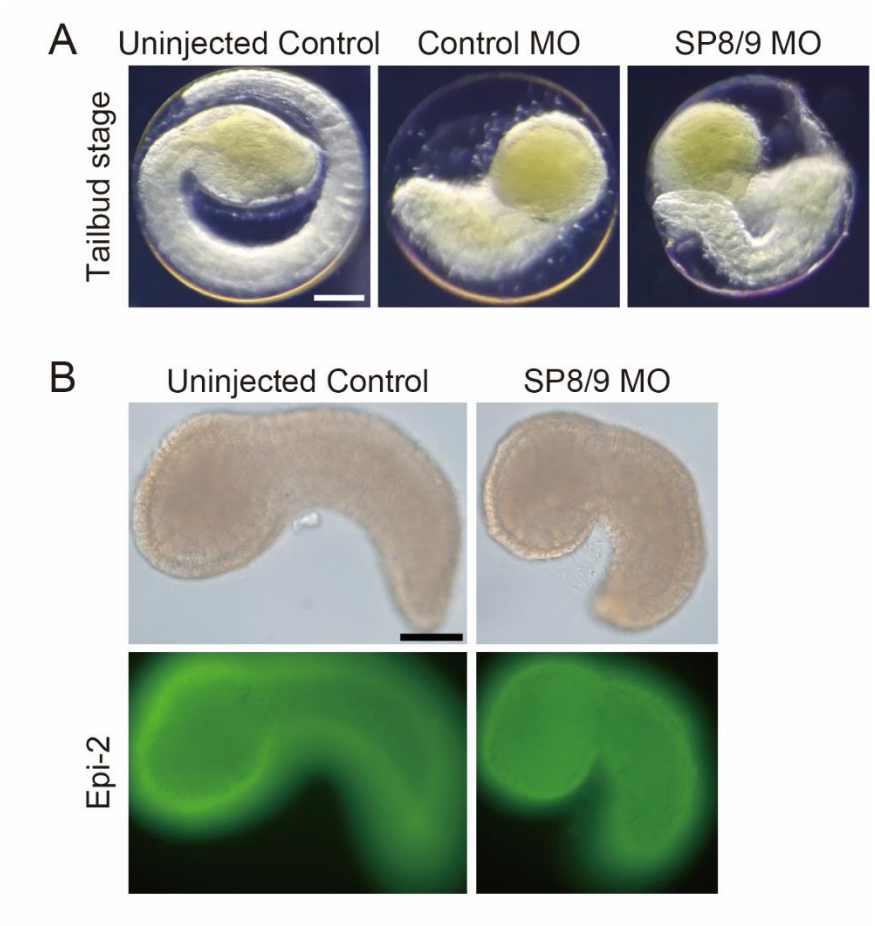

Fig. 7. SP8/9 MO-injected embryos and epidermis differentiation. **(A)** Embryos at late tailbud stage. Left to right: uninjected control, eggs injected with control MO, and eggs injected with SP8/9 MO. **(B)** The early tailbud embryos of uninjected control and SP8/9 morphant. Bottom row shows the Epi-2 antibody staining. Scale bar, 50 μm.

2-3. Conclusion

The transcription factor FoxJ-r is involved in cilia formation and neurula rotation and, consequently, in the establishment of laterality. In this study, SoxF was found to be important for blastopore closure. However, the details of its molecular functions could not be elucidated. On the other hand, SP8/9 was found to be potentially dispensable for early development. These findings provide a basis for further studies on the regulatory function of transcription factors in animal hemisphere development.

Every gene that was investigated in the present study showed expression in the animal hemisphere as early as the 16-cell stage. However, none of their knockdown embryos showed a deficiency in epidermal differentiation with regards to epithelial morphology or Epi-2 antigen expression. The transcription factors SoxB1 (Sox1/2/3) and Tfap2 are known to play essential roles in cell fate specification and in the differentiation of the ectoderm/epidermis (Liu and Satou, 2020). The expression of SoxB1 and Tfap2 also starts at the 16-cell stage in the animal hemisphere (Imai et al., 2017). In the present study, SoxB1 and Tfap2 were not investigated because they have already been extensively studied. Moreover, the peak of Tfap2 expression is found at the gastrula stage, and not in the blastula stage. The results presented in this study indicate that even transcription factor genes expressed at the cleavage stages play important roles in a range of functions, and are not limited to roles in cell fate specification.

All three genes investigated in the present study were found to be expressed in the animal hemisphere. This is likely to be due to the fact that most of the ascidian transcription factor genes that are expressed in the vegetal hemisphere during the cleavage stage have been extensively and almost comprehensively analyzed in previous studies. The fate map is more complicated in the vegetal hemisphere, which gives rise to various mesoderm and endoderm tissues (Fig. 1). In contrast, the fate map of the animal hemisphere is relatively simple, giving rise to the epidermis and brain (Fig. 1). Developmental mechanisms that operate in the animal hemisphere are also intriguing and should be clarified to understand the entire embryogenesis. Since past studies of ascidian early embryogenesis have mostly focused on the genes expressed in the vegetal hemisphere, the results presented here shed light on the development of animal hemisphere cells that has not been previously analyzed in ascidians.

Chapter3

Analysis of *cis*-Regulatory Elements of *Nodal* Gene for the Left-Sided Expression

3-1. Introduction

The spatiotemporal patterns of expression are determined by genomic *cis*-regulatory elements of genes, such as promoters, enhancers and silencers. Identification of *cis*-regulatory elements is thus a crucial step to understand the regulatory networks that regulate the biological processes (Davidson et al., 2002). With improvement of the recombinant DNA techniques, such as transgenesis of reporter gene constructs and bioinformatics, *cis*-regulatory elements analyses have been applied to uncover gene regulatory logics (Costa et al., 2017), understanding the gene expression of immune cells (Maslova et al., 2020), or even verifying the regulatory relationship in human diseases (Cherry et al., 2020). In such studies, identification of the *cis*-regulatory elements of genes that are expressed in the early embryos is important, since the spatiotemporal expression patterns of zygotic genes are directly linked to cell fate decision and differentiation.

In this topic, I focus on the *cis*-regulatory elements of the *nodal* gene of *H. roretzi*, which plays important role in the left-right axis establishment (Morokuma et al., 2002; Nishide et al., 2012). In various animals, both the external and mostly internal organization show a stereotyped left-right asymmetry. At a certain stage of embryogenesis, the L-R symmetry is broken by key events (Speder et al., 2007; Vandenberg and Levin, 2013; Blum et al., 2014; Namigai et al., 2014), which in vertebrates breaking of the L-R symmetry is carried out by motile cilia within the L-R organizer, such as in zebrafish, mouse and frog, (Nonaka et al., 1998; Okada et al., 2005). In mice, leftward nodal fluid flow is generated by the cilia in the L-R organizer node, and in the end promote left-side-specific *nodal* gene expression in the lateral plate mesoderm (Nonaka et al., 2002; Takaoka et al., 2007). The left-sided *nodal* expression then triggers the downstream *pitx2* transcription factor gene for the further left-right establishment (Morokuma et al., 2002).

In ascidians, there is no organ corresponds to the node in mice. The left-right polarity is specified by neurula rotation in ascidians instead of nodal flow in mouse. Neurulae of *H. roretzi* rotate in a counterclockwise direction at 15 h of development; this rotation stops when the left side of the embryo is oriented downwards. Consequently, contact of the left-side epidermis and vitelline membrane promotes *nodal* expression in the left-side epidermis at 2 h after neurula rotation (Nishide et al., 2012). Previous studies have shown that chemical signals from the vitelline membrane but not mechanical stimulus induce the *nodal* expression. The signal molecules can be extracted from the vitelline membrane, and are protein but not sugars. Specific fractions in gel filtration chromatography had the *nodal* promoting activity (Tanaka et al., 2019). However, trials of further protein purification and identification encountered difficulties due to the

aggregation of the vitelline membrane proteins in gel filtration chromatography. Therefore, in the present study, I approached the issue from the reverse direction by investigating the regulatory *cis*-elements of *nodal* gene that respond to the vitelline membrane signal.

The *cis*-regulatory elements of *nodal* in some vertebrates have been studied. In mice, five enhancers of *nodal* that regulate the dynamic expression during development have been identified. Deletion of the Proximal Epiblast Enhancer (PEE) would decrease the *nodal* expression in primitive streak (Vincent et al., 2003), while the Node Dependent Enhancer (NDE) is required for *nodal* expression at the left-right decision organ, the node (Adachi et al., 1999). Asymmetric Enhancer (ASE), an intronic enhancer, has shown to be essential and sufficient for the left-specific expression of *nodal* (Adachi et al., 1999; Norris et al., 2002). The Highly Bound Element (HBE), which could bind several pluripotency factors, seems to be the first activated enhancer and it might control the ASE through chromatin modifiers (Papanayotou et al., 2014). Left Side-specific Enhancer (LSE) is another enhancer that could contribute to the left-specific expression, but only weak *nodal* expression was observed and might function independently to the ASE (Adachi et al., 1999). Problem in analyses of vertebrate *nodal* genes is that nodal protein autoregulate *nodal* gene expression. This makes the situation complex. While in ascidians, *nodal* expression is not autoregulated (Nishide et al., 2012). This would make analysis of ascidian *nodal cis*-regulatory elements simpler.

In this work, the *cis*-regulatory elements of the *nodal* gene were analyzed. Inter-species conserved regions (ICRs) between *Halocynthia nodal* gene and that of another ascidian, *Ciona intestinalis*, were identified. Gene reporter assay was carried out to uncover the essential regions for the left-sided expression and the regions were analyzed by transcription factor-binding sites (TFBS) prediction tools. The protein-protein interaction of the candidate TFs that bind to these regions was further predicted and I propose a list of candidate receptor proteins which could bind to the vitelline membrane signal molecules to trigger the left-sided expression of *nodal*.

3-2. Results and Discussion

3-2-1. Genomic region that is enough for *nodal* expression

To investigate the *cis*-regulatory elements of *nodal*, a DNA sequence contain 3000 bp upstream region from the first methionine ATG (-2854 to +146) was amplified from the genomic DNA. Since in mice the ASE region in the first intron also shows the ability to regulate left-sided *nodal* expression (Adachi et al., 1999), 705 bp of the first intron (+534 to +1238) was also cloned (Fig. 8A). The 3000-Venus-Intron reporter construct, which contained a 3000 bp of the upstream and promoter region, a yellow fluorescent protein (Venus) sequence and the first intron located after the 3'UTR of Venus, was made as a starting point reporter. The Venus ORF is flanked by *nodal* 5'UTR (146 bp, predicted by the expressed sequence tag in the MAGEST database, mae42a18) and Simian virus 40 Poly-A terminator 3'UTR (248 bp).

Nodal is initially expressed during the cleavage stages in the A7.6 cells (presumptive trunk lateral cells) and in the b-line cells (descendants of b6.5, namely, b7.9-10 of the 64-cell embryo and b8.17-20 of the 110-cell embryo; nerve cord, epidermis cells and secondary muscle precursor cells), and later in left-sided epidermis cells at the neurula stage (Morokuma et al., 2002). In situ hybridization results with Venus probe of embryos injected with the 3000-Venus-Intron plasmid showed a similar expression pattern as endogenous *nodal*. Note that transient transgene expression tends to be mosaic in most animals, probably due to mosaic incorporation of reporter plasmid into nuclei. Signals were observed at the initial tailbud stage in some of the epidermis cells, while the mRNA expressed in the b-line cells were also retained (Fig. 8B, left). This prolonged retention might be due to the Venus mRNA with Simian virus 40 Poly-A terminator UTRs, which is largely stable. As a result, a construct with 3000 bp upstream and the first intron was able to drive the left-sided epidermal expression.

On the other hand, although constructs without the intron also showed in situ signals, the expression area was decreased compared to that with intron (Fig. 8B, right). This result is consistent with the previous research in mice, in which the intron region plays some important roles for the left-sided expression of *nodal* (Adachi et al., 1999).

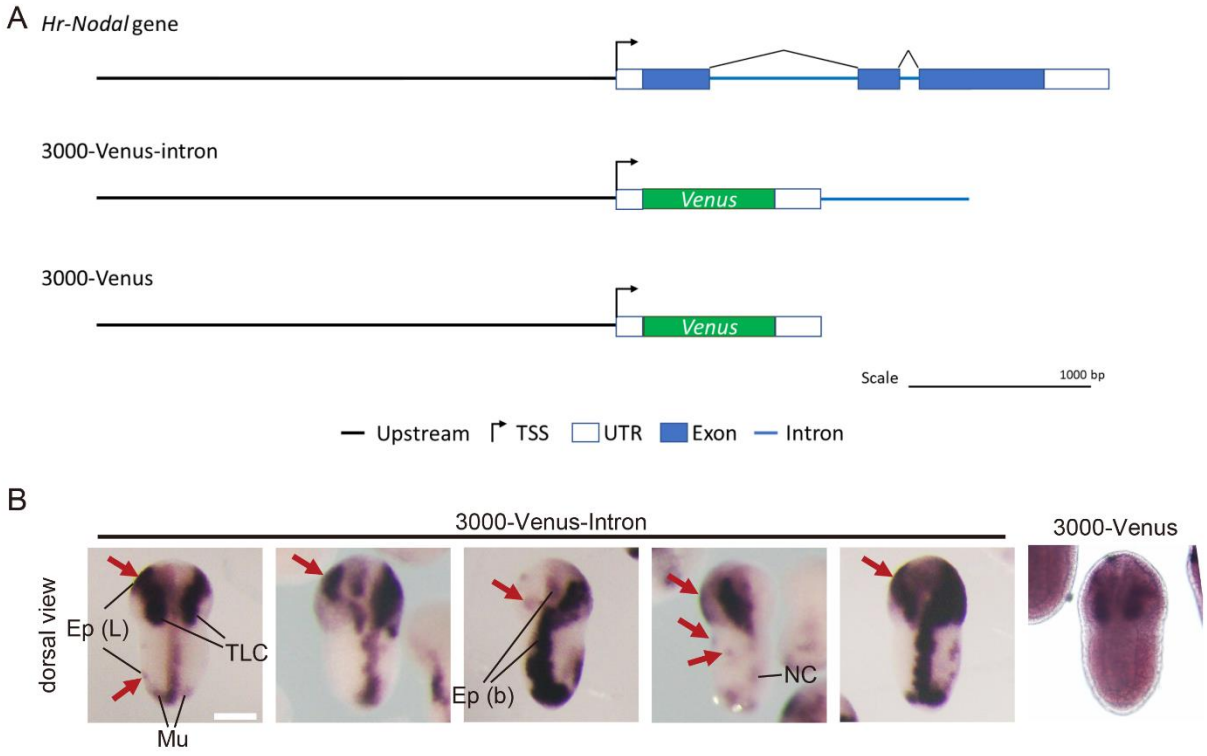

Fig. 8. Expression of the Hr-*Nodal*-Venus transgene constructs during embryonic development of *Halocynthia roretzi*. **(A)** A schematic drawing of the Venus transgene constructs. Black line: upstream sequence; arrow head: the transcription start site (TSS); white box: the UTR; blue box: exon; blue line: intron. Scale bar, 1000 bp. The Venus ORF is flanked by *nodal* 5'UTR (146 bp) and Simian virus 40 Poly-A terminator 3'UTR (248 bp). **(B)** In situ hybridization with the Venus prove at the initial tailbud stage. Left: 3000-Venus-Intron construct. Right: 3000-Venus construct. Dorsal views. Anterior is up. Expression on the left epidermis is indicated by arrows. Scale bar, 50 µm. Abbreviations: Mu, secondary muscle; TLC, Trunk lateral cells; Ep (L), Left epidermis; Ep (b), Epidermis derived from b-line cells; NC, nerve cord.

3-2-2. Inter-species conserved regions and transcription factor prediction

To identify the *cis*-regulatory regions in the 3000 bp upstream and the first intron of *nodal* gene in silico, I applied the phylogenetic footprinting, which is an efficient method to identify highly conserved regions between species in sea urchins (Yuh et al., 2002; Ragusa et al., 2012; Costa et al., 2017). Here I compared the sequence of *Halocynthia roretzi* with that of *Ciona intestinalis*, the upstream region (-3000 bp to ATG starting methionine) and the first intron (length 817 pb in *Halocynthia*). VISTA program was used for short conserved motifs scanning with setting of 70% identity in the 30 bp window parameters (Frazer et al., 2004). Two ICRs in the upstream regions and one ICR in the first intron were identified. The ICRs are located as follows: upstream ICR1: from -2707 to -2687, 21 bp; ICR2: from -963 to -937, 27 bp; intron ICR3: from +1170 to +1200, 31 bp (Fig. 9) (Table 1).

The three ICRs in C*iona* do not correspond to the three enhancer regions that had been studied previously (Khoueiry et al., 2010; Stolfi et al., 2015; Madgwick et al., 2019). The first region (-1915 to -1769) interacts with transcription factor Fox2 and induces the *nodal* expression in the b-line cells at the blastula stage. The second one (-768 to -587) seems to contribute to the epidermis expression, but the binding sites and TFs was not investigated. The last one (-434 to -164) could drive weak expression in the secondary muscle. Since any sequence of these is not conserved in the *Halocynthia*, this could be a possible reason for the different response of *nodal* expression to the vitelline membrane removal between *Halocynthia* and *Ciona* (Yoshida and Saiga, 2008).

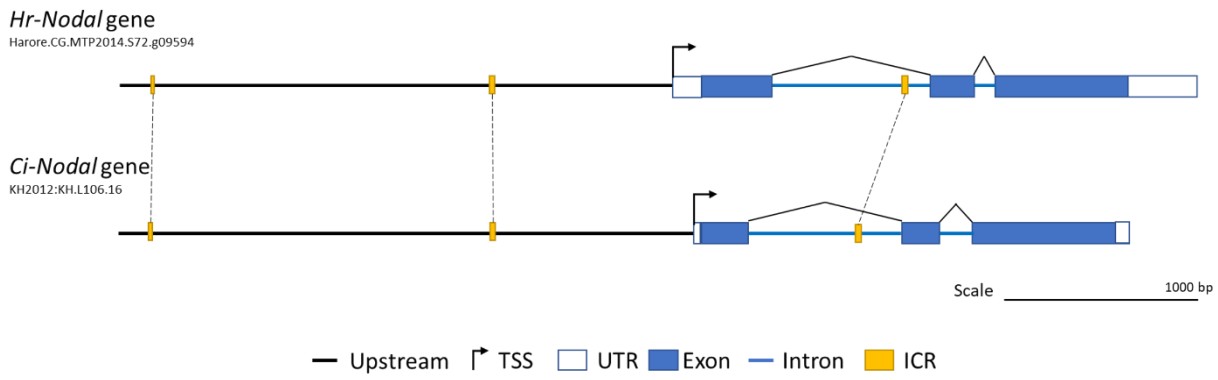

Fig. 9. Gene structure comparison of the *Hr-nodal* gene with *Ci-nodal*. The sequence of the two *nodal* genes were obtained from the Aniseed database. Black line, upstream sequence; arrow head, the transcription start site (TSS); white box, UTR; blue box, exon; blue line, intron; yellow box, ICRs. Scale bar, 1000 bp. *Hr*: *Halocynthia roretzi*; *Ci*: *Ciona intestinalis*;

Table 1. Nucleotide sequences of the inter-species conserved regions between *Halocynthia roretzi, Ciona intestinalis,* and *Phallusia mammillata*.

ICR	Length	Identify	5'-3' Sequences
ICR1			
Hr	21bp	85.7%	ATAACCAATACTGTTATGTCA
Ci			ATAACCAA-ATGGTTATGTCA
ICR2			
Hr	27bp	78.6%	AATCAAAATTGAAACAATG-AAATCATG
Ci			AATCAAAGTTGACACAAGGCAAGTTATG
ICR3			
Hr	31bp	71.4%	TCTCACTAACTACC---TTTCCATTGTTTTGAGA
Ci			TATCACT--CCACCATTGTTTCCATTGTTTATAGA

Hr: *Halocynthia roretzi*; Ci: *Ciona intestinalis*

Red letters indicate identical nucleotides.

3-2-3. Promoter replacement

Because of the weak expression of the reporter in the left epidermis, I thought that stronger promoter from other gene would improve the expression. I replaced *nodal* promoter of the 3000-Venus(-intron) construct with the promoter of *brachyury*, and made 3000-Bra-Venus (-intron) (Fig. 10A). Brachyury is a crucial transcription factor for notochord development. In *Halocynthia*, *brachyury* is expressed from blastula to tailbud stages (Hitoyoshi and Noriyuki, 1994) and its promoter region has been well studied (Matsumoto et al., 2007). Therefore, taking advantage of this strong promoter of *brachyury*, the promoter region of the 3000-Venus(-intron) (-86 to +146 of *nodal*) was replaced with the *brachyury* promoter (-82 to +20) for possible enhancement of the expression of Venus reporter (Fig 10A).

The 3000-Bra-Venus (Fig. 10B, middle, n = 11) showed stronger expression, which was similar level to the 3000-Venus-Intron (Fig. 10B, left, n = 32). Thus, the *Bra* promoter could compensate the loss of the first intron. However, when constructs contain both *brachyury* promoter and the intron region (3000-Bra-Venus-Intron) (Fig. 10B, right, n = 14), there was no improvement in the expression area compared to 3000-Venus-Intron nor 3000-Bra-Venus. Therefore, I decided to continue to use the 3000-Venus-Intron construct with the original *nodal* promoter for following study.

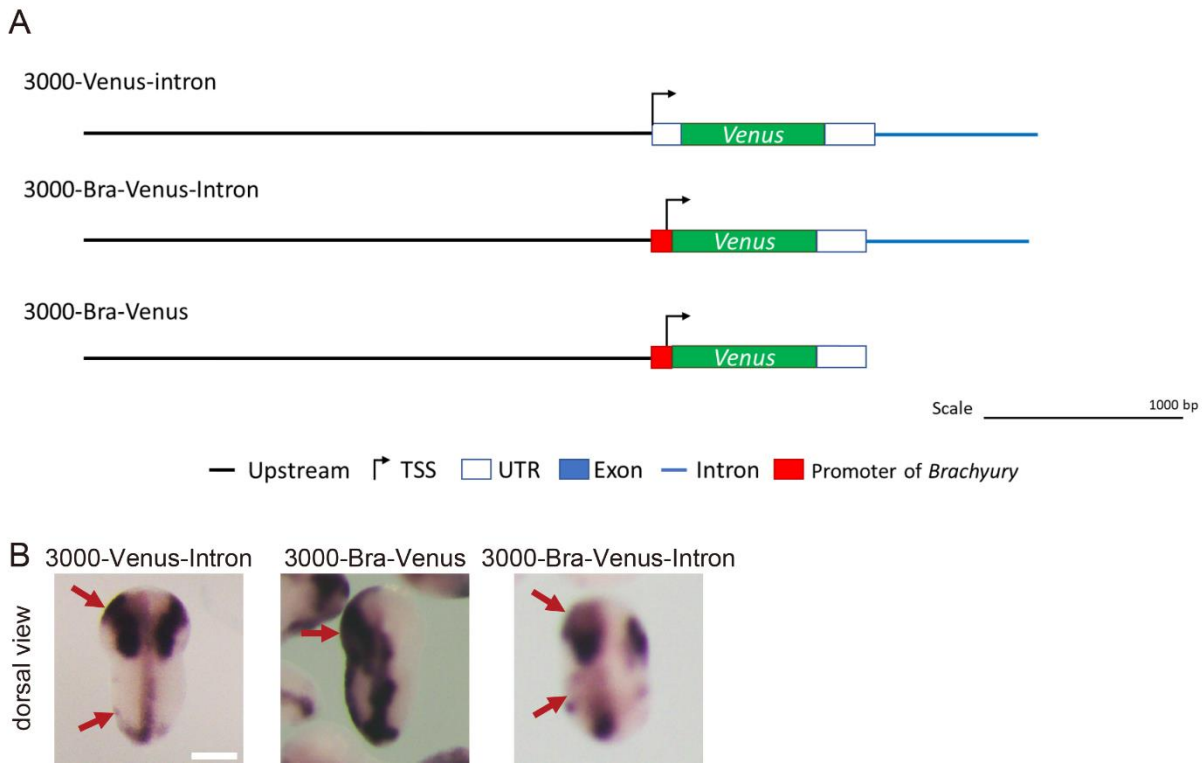

Fig. 10. Replacement of *nodal* promoter with *brachyury* promoter. **(A)** The Venus reporter constructs. Red box indicates *brachyury* promoter sequence of 101 bp-long. Scale bar, 1000 bp. **(B)** In situ hybridization of *Venus* mRNA at the initial tailbud stage. From left to right: 3000-Venus-Intron, 3000-Bra-Venus, 3000-Bra-Venus-Intorn. Dorsal view. Expression on the left epidermis is indicated by arrows. Anterior is up. Scale bar, 50 μm.

3-2-4. Analysis of upstream *cis*-regulatory elements by 5'-deletion series

In order to further analyze the upstream *cis*-regulatory elements in vivo, a series of 5'-deletion constructs with the first intron were injected. 5'-deletion removed the two ICRs one by one. Reporter *Venus* expression was monitored by in situ hybridization at the initial tailbud stage. Note that expression pattern of *Venus* was mosaic in this kind of reporter assay, and all cells that express endogenous *Nodal* did not show *Venus* expression. Thus, the expression pattern was varied between embryos. The results were shown in Fig. 11. The genomic sequence included 2065 bp upstream (-1919 to +146) and the first intron (2065-Venus-Intron) is able to drive proper reporter gene expression. There was no significant change in the expression in the left epidermis cells as well as in the cells derived from A7.6 and b-line cells (Supplementary Table S2). Therefore, 2065 upstream sequence together with the first intron is enough for proper *nodal* expression, while the removed regions (-2854 to -1920), which contain the ICR1, are dispensable.

1379-Venus-Intron construct (-1233 to +146) showed similar expression pattern in the left epidermis, while signals in the trunk lateral cells were disappeared (Fig. 11). The result indicates the deleted region (-1919 to -1234) contains the enhancer for the *nodal* expression in the A7.6 cells. 799-Venus-Intron construct (-653 to +146) and the 395-Venus intron construct (-249 to +146) still showed expression in the left epidermis and b-line derivatives. However, the proportion of embryos that showed left epidermis expression were gradually decreased to 33%. Thus, regions from -1233 to -250 including the ICR2 do not contain critical *cis*-element. -1233 to -250 seems to function as step-up enhancer to increase expression level.

302-Venus-Intron construct (-156 to +146) showed a significant reduction of the left-sided expression. Only 4% embryos showed expression in the left epidermis, and the expression were only observed in few epidermis cells but not in a large area. This deletion did not reduce the expression in the b-line derivative (Supplementary Table 2), suggesting that loss of the left-sided expression was not due to removal of the promoter region in 302-Venus-Intron construct. It is likely that the -249 to -156 region carries the crucial enhancer for *nodal* expression in left epidermis. Finally, 146-Venus-Intron construct (+1 to +146) removed the promoter, and no expression was observed in any cells.

In summary, region -1919 to -1234 contains the A-line trunk lateral cell enhancer, while the -1233 to -250 contains step-up enhancers for left epidermis expression. The crucial region for left-sided *nodal* expression located in -249 to -156 region.

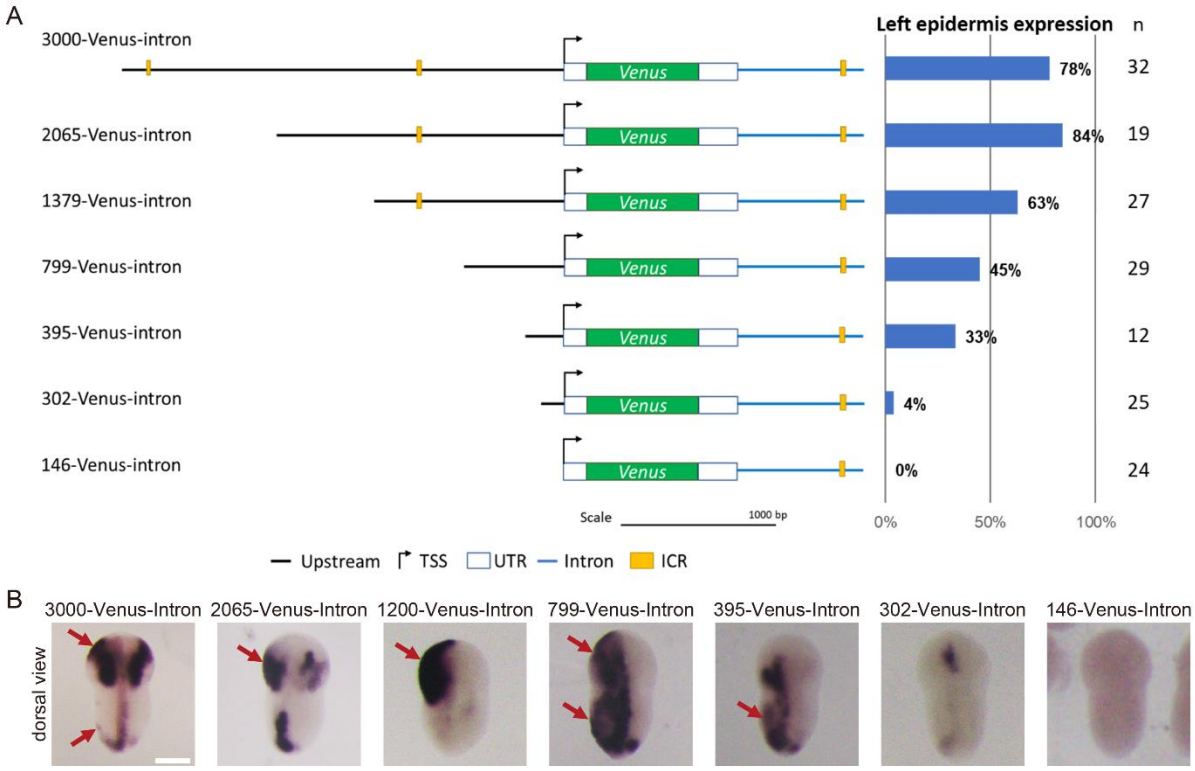

Fig. 11. Expression of the upstream 5'-deletion constructs. **(A)** Deletion series of the Venus reporter constructs. Yellow box indicates the ICR. Scale bar, 1000 bp. **(B)** In situ hybridization of *Venus* mRNA at the initial tailbud stage. Dorsal view. Anterior is up. Expression on the left epidermis is indicated by arrows. Scale bar, 50 µm.

3-2-5. Analysis of intronic *cis*-regulatory elements

In the 3-2-1 section, I showed that the first intron region is also necessary for proper reporter gene expression in the left epidermis and b-line cells but not in the A-line TLC. To analyze the first intron in more detail, a series of constructs were built (Fig. 12A). First, the ICR3 (+1169 to +1200) was eliminated in the 3000-Venus construct (3000-Venus-△ICR3). However, embryos showed no significant difference compared to 3000-Venus-Intron. Unexpectedly, the conserved regions ICR1-3 have no function in the left-sided *nodal* expression.

Next, Intron-395-Venus construct, in which the intronic region was placed in upstream of the minimal region (-249 to +146), was also built. This construct showed no ability to drive the left-sided expression of the reporter gene, as well as the construct 395-Venus (Fig. 12). The results indicate the position effect of the intron enhancer. It must be positioned downstream of an exon. The location is not precisely limited to introns since in the construct series the intronic region was placed after a single *Venus* exon.

Studies of *cis*-regulatory elements in various animals suggested that *cis*-elements were not limited to the 5' upstream regions. The intronic regions also play crucial roles in proper gene expression, such as the *PI-Tuba1a* for cilia and sensory ganglia in sea urchin (Costa et al., 2017), the *Pitx2* (one of nodal targets) for left-sided expression in ascidians (Yoshida and Saiga, 2008), or even the *SNCA* gene for Parkinson's disease in the human (Zhu et al., 2020). My results also showed that the first intronic region in the *nodal* gene is essential for the expression in the left-sided epidermis and b-line cells.

Results of the deletion series is summarized in Fig. 13. The upstream region -2854 to -1920 is not necessary for *nodal* expression. The -1919 to -1234 region contains the A-line truck lateral cell enhancer, whereas the -1233 to -250 contains step-up enhancer for left epidermis expression. Both of the -249 to -156 region and the first intron (+532 to +1142) are crucial enhancer for left-sided *nodal* expression. Losing one of them or wrong position of the intron enhancer did not drive the left-sided expression. Therefore, the minimum reporter construct in this study was the 395-Venus-Intorin, although the ICR3 is dispensable. In these deletion series, left-side enhancer activity and b-line enhancer activity were not separated (Supplementary Table S2). It is still elusive whether these two enhancers are separable.

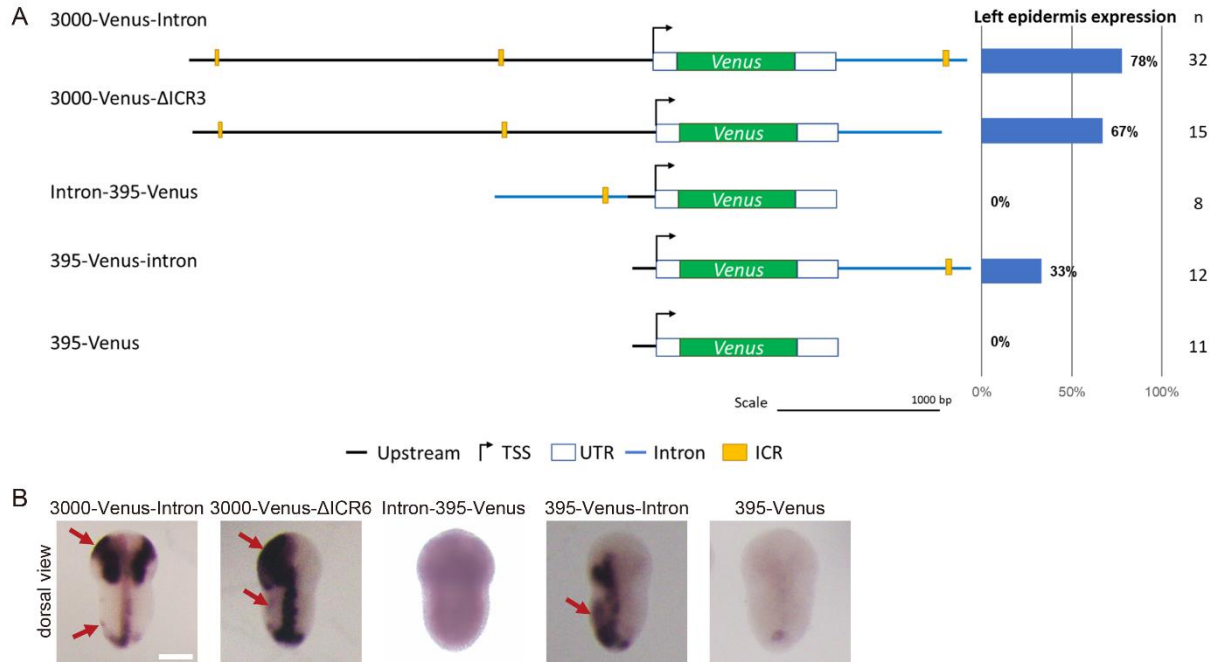

Fig. 12. Expression of the intronic deletion series. **(A)** Deletion series of the Venus reporter constructs. Scale bar, 1000 bp. **(B)** In situ hybridization of *Venus* mRNA at the initial tailbud stage. Dorsal view. Anterior is up. Scale bar, 50 µm.

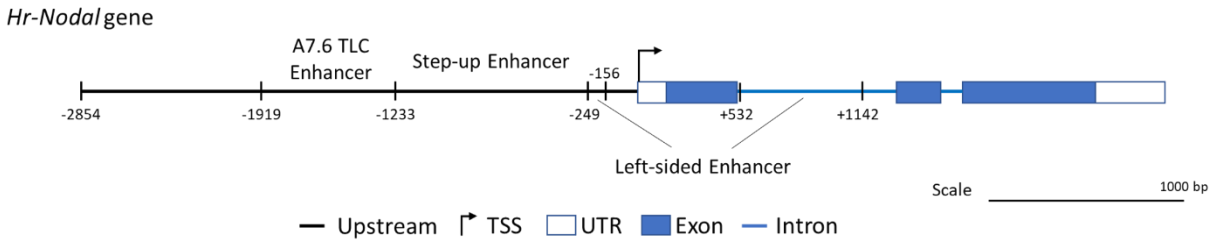

Fig. 13 Summary of results in the deletion series. Scale bar, 1000 bp.

3-2-6 In silico analyses of the -249 to -156 region and the first intron

Next, to list candidate transcription factors, the -249 to -156 upstream region and the first intron (+532 to +1142) without ICR3 were analyzed by transcription factor binding site (TFBS) prediction tool. AnimalTFDB3.0 (animal transcription factor database3.0: http://bioinfo.life.hust.edu.cn/AnimalTFDB/#!/document#gwas), a web database for classification and annotation of transcription factors, was used to evaluate the putative TFBSs (Zhang et al., 2012). Since the TFBSs of *Halocynthia* have still not been well analyzed, the whole database of the AnimalTFDB3.0, which contains 97 animal data, were used. Due to the intricate TFBS data resource, the TFs identified by the AnimalTFDB3.0 were further examined using the RNA-seq expression data of *Halocynthia* in the Aniseed database. Candidate

transcription factors should be present in *Halocynthia* gene annotation in the Aniseed database, and they should be expressed in early embryos (TFs of which the RPKM value is lower than 1 at the blastula stage and lower than 5 at the gastrula stage in the RNA-seq results were excluded). The top 32 TFBS of each region that showed high score in AnimalTFDB3.0 are listed in Table 2 (See Supplementary Table S3 for the detailed and complete list of totally 57 candidates for -249 to -156 region and 139 candidates for intron) (Supplementary Table S3 and 4 contain large data sets. So they can be downloaded at the following website. http://www.bio.sci.osaka-u.ac.jp/bio_web/lab_page/nishida/shih/index.html).

Several candidate TFs, such as TAL1, CBX, GATA family and FOX family members showed high score in binding site prediction. Among the possible TFBS identified in silico, some binding sites were corresponded to TFs that have already been studied in *Halocynthia* development. TFBSs for Fox family TFs such as FoxA and FoxO, were found in the intronic region, and FoxA has been shown to be necessary for morphogenesis of the brain and the notochord (Ikeda and Satou, 2017). Otx1 and Otx2, which are important for embryonic anterior formation (Oonuma et al., 2014), also showed higher score in the prediction results. However, as the transcriptional regulation that trigger *nodal* expression by the vitelline membrane proteins remains unknown, it is possible that the crucial TFs might be those that have not been well studied so far in ascidians, such as CBX3, SMAD family members and NPAS4.

Table 2. The presumptive TFBSs predicted in the -249 to -156 region and the first intron

TFBS	Score	TFBS	Score
-249 to -156		First intron without ICR3	
CDX2	14.8136	CBX3	14.8333
TAL1	14.7571	NPAS4	14.5102
GATA2	14.4242	MYBL2	14.3684
TCF7L2	14.1818	TP73	14.0571
GATA6	14.122	SMAD4	14.0519
ERG	13.7143	GATA6	13.6447
PDX1	13.6148	NFIC	13.4857
DMRTA1	13.6	SOX4	13.4388
GATA3	13.4697	OTX2	13.338
SMAD1	13.4697	CREBBP	13.2394
TCF4	13.4306	VDR	13.2273
BRD4	13.1286	FOXM1	13.2222
CEBPA	13.0909	FOXO1	13.2121
GATA4	13.0714	SMAD3	13.1711
HOXD11	12.8494	NKX2-2	13.0241
CTNNB1	12.7746	SIRT6	12.9571
PROX1	12.7551	BRD7	12.8831
EP300	12.6528	PPARGC1A	12.7895
EMX2	12.408	FOXA2	12.7237
PPARG	12.4	TTF2	12.7237
TP73	12.3286	TEAD3	12.6607
KDM1A	12.3	GATA4	12.6429
RELA	12.25	TCF4	12.6327
HOXD12	12.0482	POLR3A	12.6154
POLR2A	11.9605	ZNF143	12.5513
SIRT6	11.9571	SMARCB1	12.3947
NCOR1	11.9474	SUMO2/SUMO3	12.3333
CDK8	11.8182	SMAD2/SMAD3	12.3286
SMARCA4	11.8026	NFIA	12.3265
SOX17	11.8026	HIF1A	12.2727
RCOR1	11.7714	CEBPA	12.2424
CEBPB	11.6857	PITX2	12.2347

Only the top 32 TFBSs ranked by hit score in the AnimdalTFDB3.0 were shown. See Supplementary Table S2 for the complete list.

3-2-7. In silico analysis of the candidate receptor proteins that are activated by the vitelline membrane signal

To approach the goal in this study, I further analyzed the candidate TFBSs predicted in the -249 to -156 region and the first intron. For this, TFBSs that were commonly found both in the -249 to -156 region and the first intron were selected and analyzed by the web server QIAGEN GeneGlobe (https://geneglobe.qiagen.com/us/) to predict potential receptors that might affect activities of the candidate TFs using existing data. The QIAGEN GeneGlobe allows signaling transduction analysis based on published data, and provides filters for the interaction network by directionality, and for function or molecular type. In this search, 34 transmembrane proteins that might activate the candidate TFs were found. Although the databases are based on the data of mouse and human, they tentatively predicted several candidate receptor proteins. Then, receptors that was not present in *Halocynthia* gene annotation in the Aniseed database, were removed. The final 33 candidates are listed in Table 3. See also Supplementary Table S4 for details.

These receptor proteins were further evaluated with the candidate vitelline membrane proteins that were enriched in the active fractions of the vitelline membrane extract to promote *nodal* expression in the gel filtration chromatography and mass spectrometry analyses (Tanaka et al., 2019). Several proteins with Zona pellucida (ZP) domain and epidermal growth factor (EGF) domains are enriched in the active fraction, such as VC120 (vitelline coat protein 120) and VC70-like. These could be potential candidates of the vitelline membrane ligands. Among the 34 predicted receptor proteins in the present study, 6 of them also contain EGF repeats in human homolog, which are Notch, LRP6, ITGB1, LRP5, LRP1 and SELP. It has been shown that EGF-like domain has the ability of self-association interaction (Tran et al., 1997), suggesting that VC120 or VC70 would possibly interact with these receptors with the EGF-repeats and eventually induce *nodal* expression. Another possibility is that the candidate receptor functions as the EGF receptor to bind the EGF repeats of the vitelline membrane proteins. EGFR of human (P00533) contains 3 furin-like (FU) domains and a tyrosine kinase catalytic (TyrKc) domain, while one of the candidate receptors, IGF1R, has FU and TyrKc domains. Therefore, IGF1R might respond to the VC120 or VC70 protein like EGFR and drive the left epidermis expression of *nodal*.

Analysis on the predicted TFBSs in the -249 to -156 region and the first intron suggested a list of candidate receptors. These included receptors with the EGF repeats such as Notch and members of low density lipoprotein (LDL) receptor family (LRP1, 5, and 6), although LRP5 and 6 is generally known as co-receptor of Wnt signaling. IGF1R could also potentially be the receptor since it has the FU domain that could bind with EGF repeats. Further wet experiments on protein-protein interactions will be needed to fully unveil the genuine receptors and ligands.

Table 3. Candidate transmembrane receptors predicted for the candidate TFs

Receptors		
Notch	LRP5	PTCH1
ITGB2	IGF1R	TLR6
TLR2	CD40	TLR1
LRP6	ITGB4	TNFRSF11A
SFRP1	DCC	CHRNA7
CHRNA3	TNFRSF1B	SELP
IL17RB	TLR3	ADIPOR1
TNFRSF1A	CAV1	FCER2
ITGB1	ITGAM	LGR4
TLR4	ITGA6	PGRMC1
	LRP1	Tlr

The candidate receptors were ranked by corresponding TFBS score provided by the AnimalTFDB.03. See Supplementary Table S3 for details.

3-3. Conclusion

Mechanism of the left-right asymmetry establishment in *Halocynthia* has been well analyzed in the previous studies, namely, neurula rotation (Nishide et al., 2012). On the neurula rotation, the driving force is generated by the epidermis motile cilia (Yamada et al., 2019) and the role of vitelline membrane signals is to promote *nodal* expression (Tanaka et al., 2019). My research on the *cis*-regulatory elements of *nodal* gene could be the last piece of puzzle to combine above studies together, providing information to understand the whole story. The embryos of *Halocynthia* at the neurula stage first form mono-cilia on the epidermis cells, and then the wavy movement of cilia drive embryos to rotate along the anterior-posterior axis, consequently making the left-side epidermis interact with the vitelline membrane. The protein in the vitelline membrane then binds with the receptor on the epidermis cells, which could be one of the receptors proposed in this study, triggering the downstream signaling pathway, and eventually activate transcription factors. The activated TFs would bind to the -249 to -156 region and the first intron of *nodal* gene, driving the expression in the left-sided epidermis cells. This promotes the downstream events after the neurula rotation, namely, establishment of the morphological left-right asymmetry.

In most of the non-chordate deuterostome embryos or larvae, such as those of sea urchin, hemichordate and Amphioxus, cilia are used for swimming (Satoh, 2009). In contrast, Ascidians coopted the ancestral epidermal cilia to rotate neurula embryos instead of swimming because the tadpole larvae can swim with their tail (Yamada et al., 2019), which could be a crucial event during the evolution. With the progress of the evolution, in vertebrate such as zebrafish, frogs or mice, the cilia are utilized to generate node flow and drive the *nodal* expression for left-right symmetry break (Nonaka et al., 1998; Okada et al., 2005). My research further shed light on mechanisms of molecular evolution that is responsible left-sided *nodal* expression at the events of symmetry breaking and improve our understanding of mechanisms for the generation of the left-right asymmetry of organismal body in various animal species.

Chapter 4
Conclusions and Perspectives

The thesis focused on the transcriptional regulatory relationships of early embryogenesis in *Halocynthia roretzi*. Two series of research, (1) expression and functional analyses of ectodermal transcription factors and (2) *cis*-regulatory element analysis of *nodal* gene, were carried out.

(1) Expression and functional analyses of ectodermal transcription factors FoxJ-r, SoxF, and SP8/9.
Functional analyses using FoxJ-r morphants showed that they resulted in the disruption of laterality and the absence of epidermal mono-cilia, suggesting its functions in cilia formation and, consequently, in the generation of left-right asymmetry, as observed in vertebrates. SoxF knockdown resulted in incomplete epiboly by the ectoderm during gastrulation, while SP8/9 knockdown showed no phenotype until the tailbud stage in the present study, although it was expressed during blastula stages. Therefore, the function of SP8/9 is still elusive at the moment. The results on FoxJ-r and SoxF indicate that transcription factor genes expressed at the cleavage stages play roles in diverse functions, and their roles are not limited to cell fate specification.

(2) *Cis*-regulatory elements of *nodal* gene for the left sided expression.
The reporter gene assay showed that both the -249 to -156 region and the first intron of the *nodal* gene play important roles for the left-sided expression. In silico prediction of transcription factor binding sites and protein-protein interaction indicated that several receptors could be candidates to be activated by the vitelline membrane signal and could be the key molecule for the left-right asymmetry in ascidians. Knockdown experiment and antibody staining of the candidate transcription factors and receptor protein is required to confirm this. This would be the last piece of the puzzle on left-right asymmetry establishment in ascidians.

These results improve our understanding of the intricate transcriptional regulatory network in embryogenesis, and provide an important basis for future researches.

Chapter 5

Materials and Methods

Animals and embryos

Halocynthia roretzi (Chordata, Tunicata, Ascidiacea, Stolidobranchia, Pyuridae, *Halocynthia roretzi*) was mainly used as an experimental animal. *Halocynthia* were purchased from fishermen in the Aomori and Miyagi prefectures of Japan and maintained at 9°C under constant light. Spawning was triggered by holding the animals at 11-13°C overnight. Sperm and eggs were released after 8 h dark and 4 h light periods. *Halocynthia roretzi* are hermaphrodites but do not self-fertilize. Thus, the eggs were cross-fertilized using sperm from another specimen. The fertilized eggs were then cultured in natural seawater (Millipore filtered seawater) or artificial seawater (REI-SEA Marine, Iwaki) at 13°C. To prevent bacterial infection, 50 µg/ml of streptomycin and kanamycin sulfate were added to the seawater. Embryos began gastrulation at 10 h and hatched at 35 h.

RNA-seq analysis

Embryos at six stages (egg, blastula, gastrula, neurula, tailbud, and larva) were collected for RNA-seq using the acid guanidium thiocyanate-phenol-chloroform (AGPC) protocol. Two biological replicates were collected after Illumina sequencing. TopHat2 (Version 2.0.12) and Bowtie2 (version 2.2.3) were used to map the cleaned reads. Bedtools (version 2.20.1) were used to count the read number for each sample, and gene expression was normalized by the RPKM (reads per kilobase of exon per million mapped sequence reads) method. The data were deposited in the Aniseed database (https://www.aniseed.cnrs.fr/) (Dardaillon et al., 2020) and are publicly available. To profile temporal gene expression patterns, one-way ANOVA was used for one-way variance analysis. A fold change (FC) ≥ 1.5 and t-test p-value ≤ 0.05 were used to detect significant changes in the gene expression levels. A list of transcription factors encoded in *Halocynthia* genome is available on the "Regulator" database (http://www.bioinformatics.org/regulator/page.php) (Wang and Nishida, 2015).

Phylogenetic tree

The phylogenic trees were constructed using MEGA 7.0.14 (https://www.megasoftware.net/). The amino acid sequences of the three transcription factors and protein family members from model organisms were aligned using the MUSCLE program (Edgar, 2004). The trees were constructed using the neighbor-joining method, and the phylogeny was tested using Bootstrap with 500 replicates. The percentage of replicate trees in which the associated taxa clustered together are shown next to the branches of each phylogenic tree. All the amino acid sequences of the model organisms were obtained from NCBI. The sequences of another ascidian *Ciona*

intestinalis were obtained from NCBI and the *Ciona* database Ghost (http://ghost.zool.kyoto-u.ac.jp/cgi-bin/gb2/gbrowse/kh/).

Whole-mount in situ hybridization

DIG-labeled antisense RNA probes for in situ hybridization were produced as follows. The pCMVFL3 vector containing the FoxJ-r insert (MAGEST number: ma322f23; GenBank: MT787223; Aniseed gene name: Harore.CG.MTP2014.S7.g07380), SoxF insert(GenBank: MT787224; Aniseed gene name: Harore.CG.MTP2014.S339.g03722), or SP8/9 insert (MAGEST number: ma324a20; GenBank: MT787225; Aniseed gene name: Harore.CG.MTP2014.S255.g04224) was digested with restriction enzyme EcoRI.
The vector with *nodal* insert was obtained in the previous study in our laboratory (Morokuma et al., 2002), while the Venus-YFP containing vector was kindly provided by Prof. Imai in our laboratory. The *nodal* and Venus plasmids were linearized with restriction enzyme BamH1.

The antisense probes were made using T7 RNA polymerase. In situ hybridization was performed according to the standard method. Briefly, the embryos were fixed with 4% paraformaldehyde (PFA) at 4°C for 16 h. After removal of the vitelline membrane using tungsten needles, the embryos were treated with 5 μg/ml proteaseK (Sigma) at 37°C for 15 min and post-fixed with 4% PFA at room temperature for 1 h. Embryos were then hybridized in hybridization buffer containing probes at 50°C for 16 h and were treated with anti-digoxigenin-AP Fab fragments (Roche) at 4°C for another 16 h. BCIP (Roche) and NBT (Roche) were used for staining until an adequate colorization was obtained.

Microinjections

Morpholino antisense oligonucleotide (MO) and reporter constructs were microinjected into fertilized eggs. The fertilized eggs were treated with 0.05% Actinase E (Kaken Pharmaceutical) in seawater for 5 to 10 min for follicular cell removal, and then attached to a cover glass. Fast Green or Phenol Red were mixed with MO and used to fill the injection needles. The glass tubes (NARISHIGE) were pulled using a microneedle puller (Model P-97; Sutter Instrument Co.). The MOs were injected at 70–90 min after fertilization.

Morpholino antisense oligonucleotide (MO)

MO blocks the translation of target mRNAs by binding to sequence close to the start codon. The sequences of MO are as follows:
(1) FoxJ-r: 5'-TCTCAACCCGCAAGATCATAATAGT-3'
(2) SoxF: 5'-GGTCGTAATGTTCTGTTTCCATG-3'
(3) SP8/9: 5'-CACTCATGCTCATGCTTAATAATAT-3'
(4) Standard control: 5'-CCTCTTACCTCAGTTACAATTTATA-3'
Sequences corresponding to the starting methionine codons are underlined. MOs were

synthesized by Gene Tools LLC, dissolved in water, and stored at –30°C. The amounts of MO injected into each embryo were as follows: (1) FoxJ-r: 2000 pg; (2) SoxF: 500 pg; (3) SP8/9: 2000 pg. The same amount of standard control MO was injected into the control embryos.

Antibody staining

Not-1, Epi-2, and Mu-2 monoclonal antibodies (Mita-Miyazawa et al., 1987; Nishida, 1990) were used to monitor the tissue differentiation of the MO-injected embryos (morphants). The Not-1 monoclonal antibody detects notochord cells at the tailbud stage, the Epi-2 antibody stains epidermal cells after the late tailbud stage, and the Mu-2 antibody against muscle myosin detects muscle cells in tailbud embryos. The embryos were fixed with MeOH at –20°C for 10 min. The vitelline membrane was removed using tungsten needles, followed by the washing of the embryos with PBSTr (PBS with 0.1% Triton X-100). Samples were treated with the primary antibodies at 4°C for 16 h. After washing with PBSTr, they were treated with the secondary antibody (Histofine Simple Stain Mouse MAX PO(M); Nichirei Corporation) at room temperature for 1 h. After washing with PBSTr, the peroxidase activity was detected using the TSA Plus Cyanine 3 Kit (Perkin Elmer) and observed with a fluorescence microscope.

Scanning electron microscopy (SEM)

SU6600 SEM (Hitachi High-Technologies Corporation) was used for cilia observation. For fixation, the embryos were treated with 2.5% glutaraldehyde and 1% PFA in seawater at 4°C for 16 h (Nishide et al., 2012). After removing the vitelline membrane, the embryos were dehydrated in 100% ethanol, critical-point dried in a Samdri®-PVT-3D machine (Tousimis Research Corporation), and coated with a thin layer of gold using a JFC-1500 Ion Sputtering Device (JEOL).

Generation of *cis*-regulatory reporter constructs

The 5’ deletion construct series were generated by PCR amplification and ligation with In-Fusion® HD Cloning Kit (Clontech/ Takara: https://catalog.takara-bio.co.jp/product/basic_info.php?unitid=U100006645). genomic DNA of 3000 bp upstream and the first intron of the *nodal* gene (Gene ID in the Aniseed Database: Harore.CG.MTP2014.S72.g09594@ https://www.aniseed.cnrs.fr/ : GenBank accession No.; BAC11909.1) were amplified from sperm DNA of *H. roretzi*, and inserted into a Venus containing pBluescript SK(+) vector.

For PCR amplification, 25 µl of 2 x PCR Buffer for KOD FX (Toyobo), 10 µl of 2 mM dNTPs (Toyobo), 5 µl of 2 µM Primer F, 5 µl of 2 µM Primer R, 0.5 µl of plasmid, 3.5 µl of DW, and 1 µl of KOD FX Neo (Toyobo) were mixed. The PCR was processed under following condition: 94°C for 2 min, (98°C for 10 sec, (Tm of primers-5°C) for 30 sec, 68°C for 30 sec x n Kbps of target sequence) for 35 cycles and terminated at 10°C. For cloning, 2.5 µl of PCR

product was mixed with 1 µl of Cloning enhancer (Takara) at 37°C for 15 min, and then at 80°C for 15min.

For ligation, 1 µl of the insert DNA, 1 µl of the vector, 1 µl of Infusion mix (Takara) and 2 µl water were mixed and processed at 50°C for 15 min. The infusion product was then transformed into DH5α *E. coli*.

The 5' deletion constructs were generated by the same method based on the 3000-Venus-Intron construct. The promoter of *Brachyury* was amplified from the construct of the previous study in our laboratory (Matsumoto et al., 2007). The primers used in this study are listed in Table S1.

The concentration of constructs for microinjection were 20 ng/µl.

Comparison of genomic sequences and TFBS analysis

The sequences of *Hr-nodal* and *Ci-nodal* were obtained from the Aniseed database (https://www.aniseed.cnrs.fr/). Identification of the interspecific conserved regions of the genomic sequences was performed by the VISTA platform (http://genome.lbl.gov/vista/index.shtml) (Frazer et al., 2004). The window size was set to 30 bp with 70% identity.

The prediction of TFBS in the relevant genomic DNA region was performed by the AnimalTFDBs 3.0 (http://bioinfo.life.hust.edu.cn/AnimalTFDB/) using the whole 97 animal genomes database integrated from HOCOMOCO, TRANSFC, JASPR and CISBP databases (Zhang et al., 2012).

Protein interaction network analysis of candidate TFs and identification of receptor proteins

The QIAGEN GeneGlobe web server (https://geneglobe.qiagen.com/us/) was used for identification of candidate receptor proteins. Interaction network of provided TF was shown in the "Explore" section, and was filtered by the following conditions: "upstream" for directionality and "transmembrane receptor" for molecular type.

REFERENCES

Aamar E, Dawid I B (2008). Isolation and expression analysis of foxj1 and foxj1.2 in zebrafish embryos. Int J Dev Biol 52: 985-991.

Adachi H, Saijoh Y, Mochida K, Ohishi S, Hashiguchi H, Hirao A et al. (1999). Determination of left/right asymmetric expression of nodal by a left side-specific enhancer with sequence similarity to a lefty-2 enhancer. Genes Dev 13: 1589-1600.

Ahmed N, Howard L, Woodland H R (2004). Early endodermal expression of the Xenopus Endodermin gene is driven by regulatory sequences containing essential Sox protein-binding elements. Differentiation 72: 171-184.

Bell S M, Schreiner C M, Waclaw R R, Campbell K, Potter S S, Scott W J (2003). Sp8 is crucial for limb outgrowth and neuropore closure. Proc Natl Acad Sci U S A 100: 12195-12200.

Blum M, Feistel K, Thumberger T, Schweickert A (2014). The evolution and conservation of left-right patterning mechanisms. Development 141: 1603-1613.

Bouwman P, Philipsen S (2002). Regulation of the activity of Sp1-related transcription factors. Mol Cell Endocrinol 195: 27-38.

Chan T M, Chao C H, Wang H D, Yu Y J, Yuh C H (2009). Functional analysis of the evolutionarily conserved cis-regulatory elements on the sox17 gene in zebrafish. Dev Biol 326: 456-470.

Cherry T J, Yang M G, Harmin D A, Tao P, Timms A E, Bauwens M et al. (2020). Mapping the cis-regulatory architecture of the human retina reveals noncoding genetic variation in disease. Proc Natl Acad Sci U S A 117: 9001-9012.

Costa S, Nicosia A, Cuttitta A, Gianguzza F, Ragusa M A (2017). An Intronic cis-Regulatory Element Is Crucial for the Alpha Tubulin Pl-Tuba1a Gene Activation in the Ciliary Band and Animal Pole Neurogenic Domains during Sea Urchin Development. PLoS One 12: e0170969.

Crowther R J, Whittaker J R (1992). Structure of the caudal neural tube in an ascidian larva: vestiges of its possible evolutionary origin from a ciliated band. J Neurobiol 23: 280-292.

Dardaillon J, Dauga D, Simion P, Faure E, Onuma T A, DeBiasse M B et al. (2020). ANISEED 2019: 4D exploration of genetic data for an extended range of tunicates. Nucleic Acids Res 48: D668-D675.

Davidson E H, Rast J P, Oliveri P, Ransick A, Calestani C, Yuh C H et al. (2002). A genomic regulatory network for development. Science 295: 1669-1678.

Dichtel-Danjoy M L, Caldeira J, Casares F (2009). SoxF is part of a novel negative-feedback loop in the wingless pathway that controls proliferation in the Drosophila wing disc. Development 136: 761-769.

Didon L, Zwick R K, Chao I W, Walters M S, Wang R, Hackett N R et al. (2013). RFX3 modulation of FOXJ1 regulation of cilia genes in the human airway epithelium. Respir Res 14: 70.

Edgar R C (2004). MUSCLE: multiple sequence alignment with high accuracy and high

throughput. Nucleic Acids Res 32: 1792-1797.

Francois M, Koopman P, Beltrame M (2010). SoxF genes: Key players in the development of the cardio-vascular system. Int J Biochem Cell Biol 42: 445-448.

Frazer K A, Pachter L, Poliakov A, Rubin E M, Dubchak I (2004). VISTA: computational tools for comparative genomics. Nucleic Acids Res 32: W273-279.

Haro E, Delgado I, Junco M, Yamada Y, Mansouri A, Oberg K C et al. (2014). Sp6 and Sp8 transcription factors control AER formation and dorsal-ventral patterning in limb development. PLoS Genet 10: e1004468.

Hitoyoshi Y, Noriyuki S (1994). An ascidian homolog of the mouse *brachyury* (T) gene is expressed exculsively in notochord cells at the fate restricted stage. Dev Growth Differ 36.

Ikeda T, Satou Y (2017). Differential temporal control of Foxa.a and Zic-r.b specifies brain versus notochord fate in the ascidian embryo. Development 144: 38-43.

Imai K S, Hino K, Yagi K, Satoh N, Satou Y (2004). Gene expression profiles of transcription factors and signaling molecules in the ascidian embryo: towards a comprehensive understanding of gene networks. Development 131: 4047-4058.

Imai K S, Levine M, Satoh N, Satou Y (2006). Regulatory blueprint for a chordate embryo. Science 312: 1183-1187.

Imai K S, Hikawa H, Kobayashi K, Satou Y (2017). Tfap2 and Sox1/2/3 cooperatively specify ectodermal fates in ascidian embryos. Development 144: 33-37.

Imai K S, Kobayashi K, Kari W, Rothbacher U, Ookubo N, Oda-Ishii I et al. (2020). Gata is ubiquitously required for the earliest zygotic gene transcription in the ascidian embryo. Dev Biol 458: 215-227.

Kawakami Y, Esteban C R, Matsui T, Rodriguez-Leon J, Kato S, Izpisua Belmonte J C (2004). Sp8 and Sp9, two closely related buttonhead-like transcription factors, regulate Fgf8 expression and limb outgrowth in vertebrate embryos. Development 131: 4763-4774.

Khoueiry P, Rothbacher U, Ohtsuka Y, Daian F, Frangulian E, Roure A et al. (2010). A cis-regulatory signature in ascidians and flies, independent of transcription factor binding sites. Curr Biol 20: 792-802.

Kim K, Kim I K, Yang J M, Lee E, Koh B I, Song S et al. (2016). SoxF Transcription Factors Are Positive Feedback Regulators of VEGF Signaling. Circ Res 119: 839-852.

Konno A, Kaizu M, Hotta K, Horie T, Sasakura Y, Ikeo K et al. (2010). Distribution and structural diversity of cilia in tadpole larvae of the ascidian Ciona intestinalis. Dev Biol 337: 42-62.

Kumano G, Negoro N, Nishida H (2014). Transcription factor Tbx6 plays a central role in fate determination between mesenchyme and muscle in embryos of the ascidian, Halocynthia roretzi. Dev Growth Differ 56: 310-322.

Levin M, Johnson R L, Stern C D, Kuehn M, Tabin C (1995). A molecular pathway determining left-right asymmetry in chick embryogenesis. Cell 82: 803-814.

Li X, Floriddia E M, Toskas K, Chalfouh C, Honore A, Aumont A et al. (2018). FoxJ1 regulates

spinal cord development and is required for the maintenance of spinal cord stem cell potential. Exp Cell Res 368: 84-100.

Liu B, Satou Y (2019). Foxg specifies sensory neurons in the anterior neural plate border of the ascidian embryo. Nat Commun 10: 4911.

Liu B, Satou Y (2020). The genetic program to specify ectodermal cells in ascidian embryos. Dev Growth Differ 62: 301-310.

Madgwick A, Magri M S, Dantec C, Gailly D, Fiuza U M, Guignard L et al. (2019). Evolution of embryonic cis-regulatory landscapes between divergent Phallusia and Ciona ascidians. Dev Biol 448: 71-87.

Makabe K W, Nishida H (2012). Cytoplasmic localization and reorganization in ascidian eggs: role of postplasmic/PEM RNAs in axis formation and fate determination. Wiley Interdiscip Rev Dev Biol 1: 501-518.

Maslova A, Ramirez R N, Ma K, Schmutz H, Wang C, Fox C et al. (2020). Deep learning of immune cell differentiation. Proc Natl Acad Sci U S A 117: 25655-25666.

Matsumoto J, Kumano G, Nishida H (2007). Direct activation by Ets and Zic is required for initial expression of the Brachyury gene in the ascidian notochord. Dev Biol 306: 870-882.

Mita-Miyazawa I, Nishikata T, Satoh N (1987). Cell- and tissue-specific monoclonal antibodies in eggs and embryos of the ascidian Halocynthia roretzi. Development 99: 155-162.

Montague T G, Gagnon J A, Schier A F (2018). Conserved regulation of Nodal-mediated left-right patterning in zebrafish and mouse. Development 145.

Morokuma J, Ueno M, Kawanishi H, Saiga H, Nishida H (2002). HrNodal, the ascidian nodal-related gene, is expressed in the left side of the epidermis, and lies upstream of HrPitx. Dev Genes Evol 212: 439-446.

Namigai E K, Kenny N J, Shimeld S M (2014). Right across the tree of life: the evolution of left-right asymmetry in the Bilateria. Genesis 52: 458-470.

Nishida H (1990). Determinative mechanisms in secondary muscle lineages of ascidian embryos: development of muscle-specific features in isolated muscle progenitor cells. Development 108: 559-568.

Nishida H (2005). Specification of embryonic axis and mosaic development in ascidians. Dev Dyn 233: 1177-1193.

Nishida H (2012). The maternal muscle determinant in the ascidian egg. Wiley Interdiscip Rev Dev Biol 1: 425-433.

Nishida H, Stach T (2014). Cell lineages and fate maps in tunicates: conservation and modification. Zoolog Sci 31: 645-652.

Nishide K, Mugitani M, Kumano G, Nishida H (2012). Neurula rotation determines left-right asymmetry in ascidian tadpole larvae. Development 139: 1467-1475.

Nonaka S, Tanaka Y, Okada Y, Takeda S, Harada A, Kanai Y et al. (1998). Randomization of left-right asymmetry due to loss of nodal cilia generating leftward flow of extraembryonic fluid

in mice lacking KIF3B motor protein. Cell 95: 829-837.

Nonaka S, Shiratori H, Saijoh Y, Hamada H (2002). Determination of left-right patterning of the mouse embryo by artificial nodal flow. Nature 418: 96-99.

Norris D P, Brennan J, Bikoff E K, Robertson E J (2002). The Foxh1-dependent autoregulatory enhancer controls the level of Nodal signals in the mouse embryo. Development 129: 3455-3468.

Okada Y, Takeda S, Tanaka Y, Belmonte J I, Hirokawa N (2005). Mechanism of nodal flow: a conserved symmetry breaking event in left-right axis determination. Cell 121: 633-644.

Oonuma K, Hirose D, Takatori N, Saiga H (2014). Analysis of the Transcription Regulatory Mechanism of Otx During the Development of the Sensory Vesicle in Ciona intestinalis. Zoolog Sci 31: 565-572.

Papanayotou C, Benhaddou A, Camus A, Perea-Gomez A, Jouneau A, Mezger V et al. (2014). A novel nodal enhancer dependent on pluripotency factors and smad2/3 signaling conditions a regulatory switch during epiblast maturation. PLoS Biol 12: e1001890.

Ragusa M A, Longo V, Emanuele M, Costa S, Gianguzza F (2012). In silico characterization of the neural alpha tubulin gene promoter of the sea urchin embryo Paracentrotus lividus by phylogenetic footprinting. Mol Biol Rep 39: 2633-2644.

Ristoratore F, Spagnuolo A, Aniello F, Branno M, Fabbrini F, Di Lauro R (1999). Expression and functional analysis of Cititf1, an ascidian NK-2 class gene, suggest its role in endoderm development. Development 126: 5149-5159.

Satoh N (2009). An advanced filter-feeder hypothesis for urochordate evolution. Zoolog Sci 26: 97-111.

Satou Y, Imai K S, Satoh N (2001). Early embryonic expression of a LIM-homeobox gene Cs-lhx3 is downstream of beta-catenin and responsible for the endoderm differentiation in Ciona savignyi embryos. Development 128: 3559-3570.

Sim D L, Chow V T (1999). The novel human HUEL (C4orf1) gene maps to chromosome 4p12-p13 and encodes a nuclear protein containing the nuclear receptor interaction motif. Genomics 59: 224-233.

Spagnuolo A, Di Lauro R (2002). Cititf1 and endoderm differentiation in Ciona intestinalis. Gene 287: 115-119.

Speder P, Petzoldt A, Suzanne M, Noselli S (2007). Strategies to establish left/right asymmetry in vertebrates and invertebrates. Curr Opin Genet Dev 17: 351-358.

Stolfi A, Ryan K, Meinertzhagen I A, Christiaen L (2015). Migratory neuronal progenitors arise from the neural plate borders in tunicates. Nature 527: 371-374.

Takaoka K, Yamamoto M, Hamada H (2007). Origin of body axes in the mouse embryo. Curr Opin Genet Dev 17: 344-350.

Tam P P, Kanai-Azuma M, Kanai Y (2003). Early endoderm development in vertebrates: lineage differentiation and morphogenetic function. Curr Opin Genet Dev 13: 393-400.

Tanaka Y, Yamada S, Connop S L, Hashii N, Sawada H, Shih Y et al. (2019). Vitelline membrane proteins promote left-sided nodal expression after neurula rotation in the ascidian, Halocynthia roretzi. Dev Biol 449: 52-61.

Tian T, Zhao L, Zhang M, Zhao X, Meng A (2009). Both foxj1a and foxj1b are implicated in left-right asymmetric development in zebrafish embryos. Biochem Biophys Res Commun 380: 537-542.

Tran H, VanDusen W J, Argraves W S (1997). The self-association and fibronectin-binding sites of fibulin-1 map to calcium-binding epidermal growth factor-like domains. J Biol Chem 272: 22600-22606.

Treichel D, Schock F, Jackle H, Gruss P, Mansouri A (2003). mBtd is required to maintain signaling during murine limb development. Genes Dev 17: 2630-2635.

Vandenberg L N, Levin M (2013). A unified model for left-right asymmetry? Comparison and synthesis of molecular models of embryonic laterality. Dev Biol 379: 1-15.

Vincent S D, Dunn N R, Hayashi S, Norris D P, Robertson E J (2003). Cell fate decisions within the mouse organizer are governed by graded Nodal signals. Genes Dev 17: 1646-1662.

Wang K, Nishida H (2015). REGULATOR: a database of metazoan transcription factors and maternal factors for developmental studies. BMC Bioinformatics 16: 114.

Yamada S, Tanaka Y, Imai K S, Saigou M, Onuma T A, Nishida H (2019). Wavy movements of epidermis monocilia drive the neurula rotation that determines left-right asymmetry in ascidian embryos. Dev Biol 448: 173-182.

Yoshida K, Saiga H (2008). Left-right asymmetric expression of Pitx is regulated by the asymmetric Nodal signaling through an intronic enhancer in Ciona intestinalis. Dev Genes Evol 218: 353-360.

Yu X, Ng C P, Habacher H, Roy S (2008). Foxj1 transcription factors are master regulators of the motile ciliogenic program. Nat Genet 40: 1445-1453.

Yuh C H, Brown C T, Livi C B, Rowen L, Clarke P J, Davidson E H (2002). Patchy interspecific sequence similarities efficiently identify positive cis-regulatory elements in the sea urchin. Dev Biol 246: 148-161.

Zhang H M, Chen H, Liu W, Liu H, Gong J, Wang H et al. (2012). AnimalTFDB: a comprehensive animal transcription factor database. Nucleic Acids Res 40: D144-149.

Zhu S G, Lu H, Mao M, Li Z F, Cui L, Ovlyakulov B et al. (2020). The cis-Regulatory Element of SNCA Intron 4 Modulates Susceptibility to Parkinson's Disease in Han Chinese. Front Genet 11: 590365.

PUBLICATIONS

Yu Shih, Kai Wang, Gaku Kumano, and Hiroki Nishida

Expression and Functional Analyses of Ectodermal Transcription Factors FoxJ-r, SoxF, and SP8/9 in Early Embryos of the Ascidian *Halocynthia roretzi*

Zoological Science in press. (2021).

doi: 10.2108/zs200128

Yuka Tanaka, Shiori Yamada, Samantha L Connop, Noritaka Hashii, Hitoshi Sawada, Yu Shih, Hiroki Nishida.

Vitelline membrane proteins promote left-sided *nodal* expression after neurula rotation in the ascidian, *Halocynthia roretzi*

Developmental Biology 449, 52-61. (2019).

doi: 10.1016/j.ydbio.2019.01.016

Lawrence Yu-Min Liu, Min-Hsuan Lin, Yu Shih, Yung-Jen Chuang.

Bioinformatics analysis of hereditary disease gene set to identify key modulators of myocardial remodeling during heart regeneration in zebrafish

BICOB-2020 Proceedings of the 12th International Conference on Bioinformatics and Computational Biology, 70, 226-237. (2020)

doi: 10.29007/9p1h

PRESENTATIONS

2018 年 10 月、第 4 回ホヤ研究会、仙台、口頭発表

Shih Yu, Wang Kai, Hiroki Nishida.
Expression and functional analyses of the five transcription factors in the *Halocynthia* embryos.

2019 年 5 月、2019 年度 日本動物学会 近畿支部研究発表会、神戸、口頭発表

Shih Yu, Wang Kai, Hiroki Nishida.
Expression and functional analyses of the four ectodermal transcription factors in the ascidian, *Halocynthia* embryos

2019 年 7 月 10th International Tunicate Meeting (第 10 回国際被嚢類学会), France, serial number P25, Poster

Shih Yu, Wang Kai, Hiroki Nishida
Expression and functional analyses of the four ectodermal transcription factors in the ascidian, *Halocynthia* embryos

ACKNOWLEDGEMENTS

This thesis is a summary of my all researches in Laboratory of Developmental Biology, Department of Biological Science, Graduate School of Science, Osaka University.

First of all, I would like to express my gratitude to Prof. Hiroki NISHIDA, who supported me to finish my researches and taught me how to be a researcher. I really enjoyed the research environment he created in our laboratory. The skillful guidance, innovative ideas and stoic patience of Prof. Hiroki NISHIDA are greatly appreciated.

I would like to acknowledge the valuable advice from Prof. Kaoru IMAI and Prof. Takeshi ONUMA, who contributed to many discussions that helped to shape my researches and resolving technical difficulties.

I would like to appreciate Prof. Takeshi MATSUNO, Prof. Gaku KUMANO and Dr. Kai WANG for checking the manuscript and giving the comments and suggestions.

This work would not be completed without the support of all the laboratory members. It was a great pleasure to do experiment with them and I appreciate their ideas, help and great Japanese humor.

I would also like to thank the members of the Asamushi Research Center for Marine Biology and the Onagawa Field Center for their help in collecting live ascidian adults and the Seto Marine Biological Laboratory for their help in maintaining the animals.

Last but not least, my deepest appreciation belongs to my family for their patience and undersetting.

SUPPLEMENTARY MATERIALS

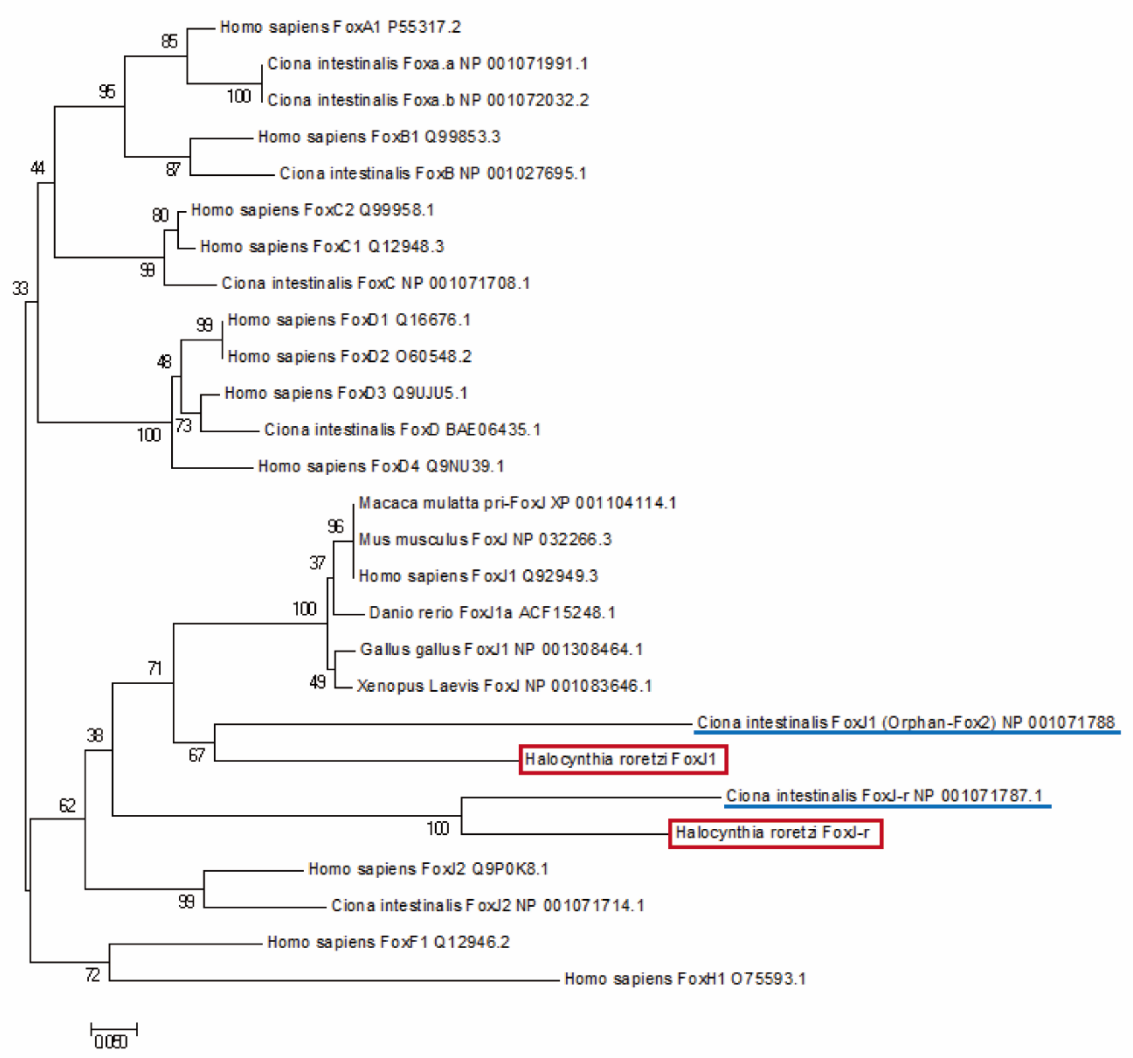

Supplementary Figure S1. Phylogenetic tree of Fox family transcription factors. Phylogenetic tree of Fox family transcription factors was generated by MEGA-7 software. The trees were constructed with the Neighbor-Joining method and the phylogeny was tested by the Bootstrap with 500 replicates. The percentages of replicate trees in which the associated taxa clustered together are shown next to the branches of each phylogenic tree. Sequences except for *Halocynthia* FoxJ-r and FoxJ1 were obtained from NCBI protein database using BLAST. Sequences of the DNA-binding Fox domain were compared.

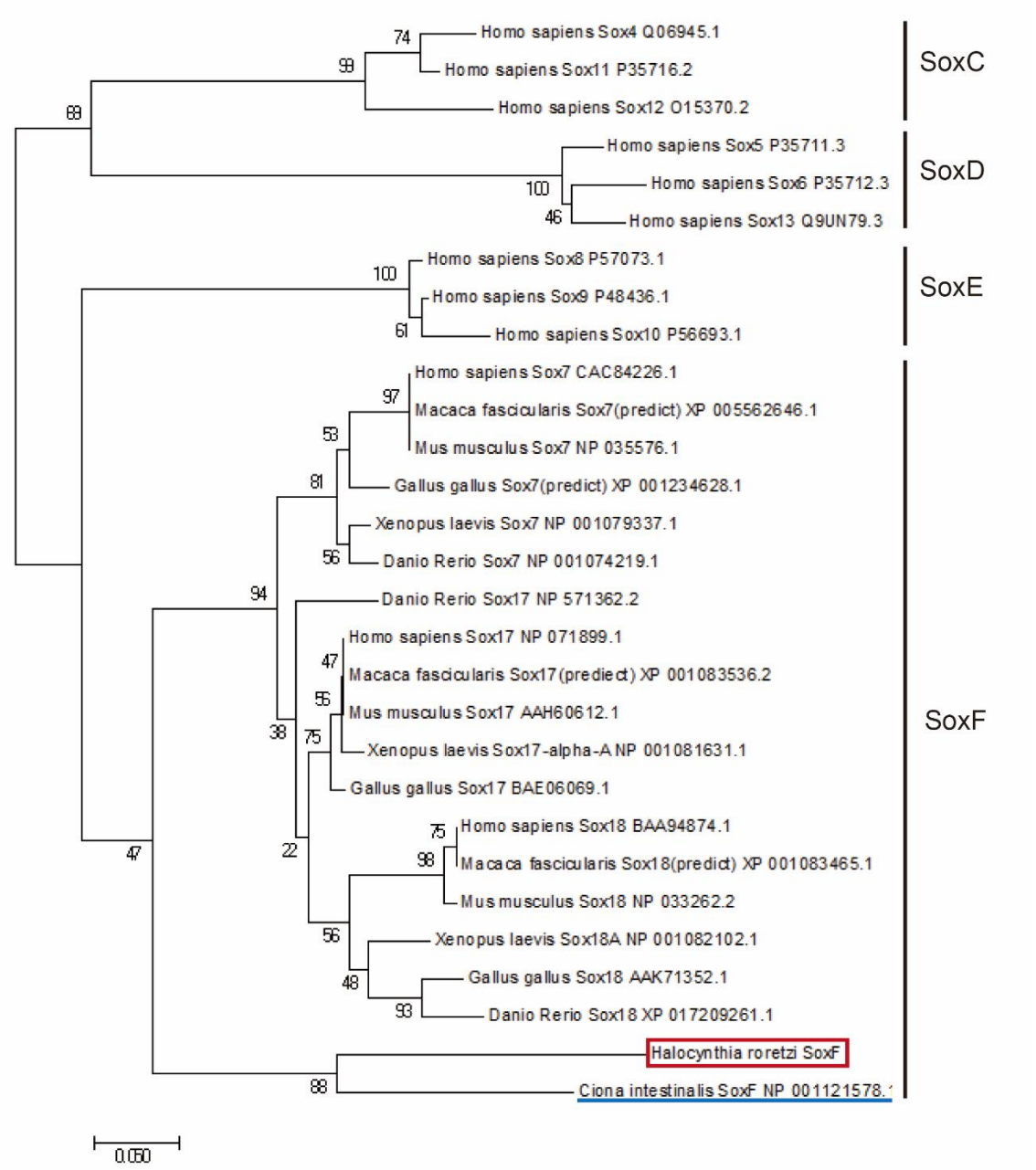

Supplementary Figure S2. Phylogenetic tree of SRY-related HMG-box (SoxF) family transcription factors. Sequences except for *Halocynthia* SoxF were obtained from NCBI protein database using BLAST. Sequences of DNA-binding HMG-box domain were compared.

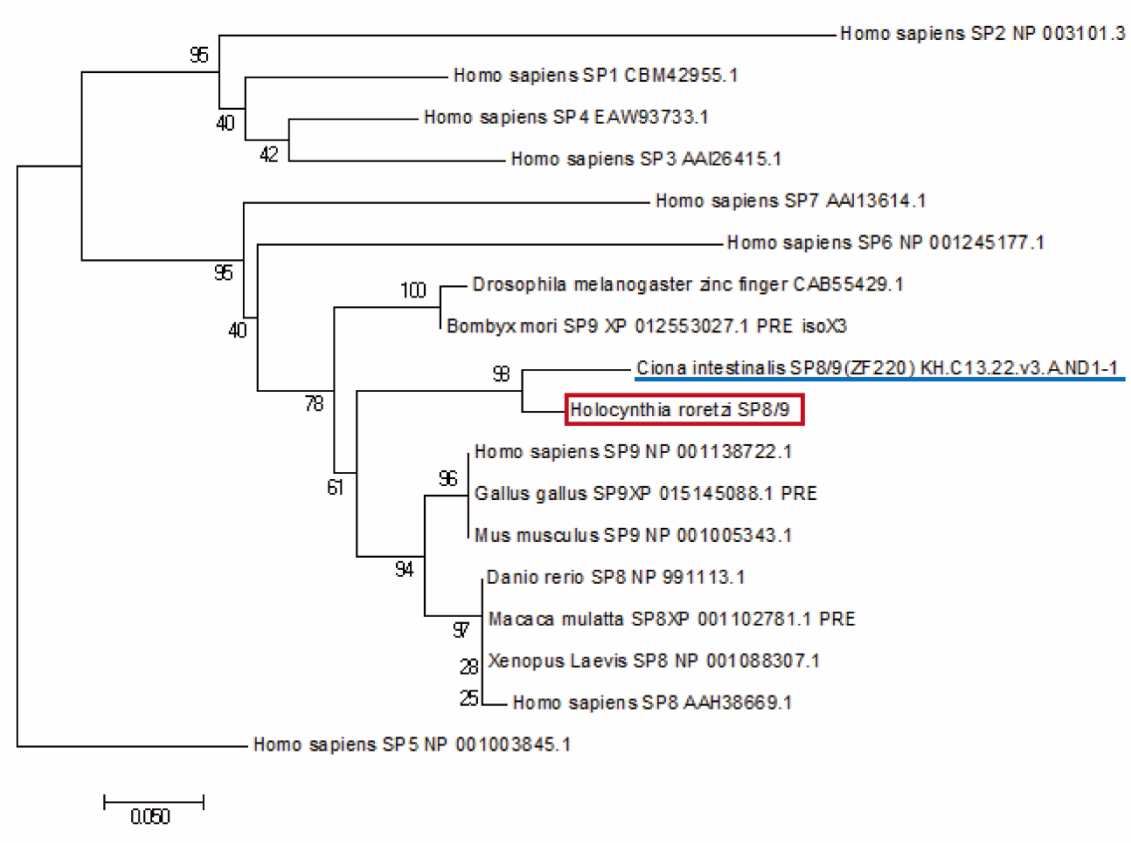

Supplementary Figure S3. Phylogenetic tree of SP family transcription factors. Sequences except for *Halocynthia* SP8/9 were obtained from NCBI protein database using BLAST. Sequences of Btd box, SP domain, and zinc finger motifs were compared.

Supplementary Table S1. Primer set of reporter constructs

5' deletion constructs		**5'-3' Sequences**
3000 bp	Forward	CAATAGGAATGTGGAATATGTCGC
2065 bp	Forward	AGAAGCATGGGCGCTAAGTA
1379 bp	Forward	CGTTGTCGTTACGCATACACTG
799 bp	Forward	GATTGCTCGTGAACATCTG
395 bp	Forward	GGTGCGACCGTTAATTATG
302 bp	Forward	ATTCTTTGTTTGCCCTCG
146 bp	Forward	ATTTTTAATTTCAATGAGGAAGAGC
Shared	Reverse	TTTAGAAATAAGTTTTAGCAGGTAGGTAG
Other regions		**5'-3' Sequences**
Intron	Forward	AATCCCTGAGAGTCACTGAG
	Reverse	CAGGAAGCAGGTTGATGTC
ΔICR6	Forward	AATCCCTGAGAGTCACTGAG
	Reverse	GCGGTCAATAGCTACTGC
***Brachyury* promoter**	Forward	TTGGTGCGATAGTTCGAG
	Reverse	TTTAGAAATAAGTTTTAGCAGGTAGGTAG

Supplementary Table S2. In situ hybridization results of 5'-deletion constructs

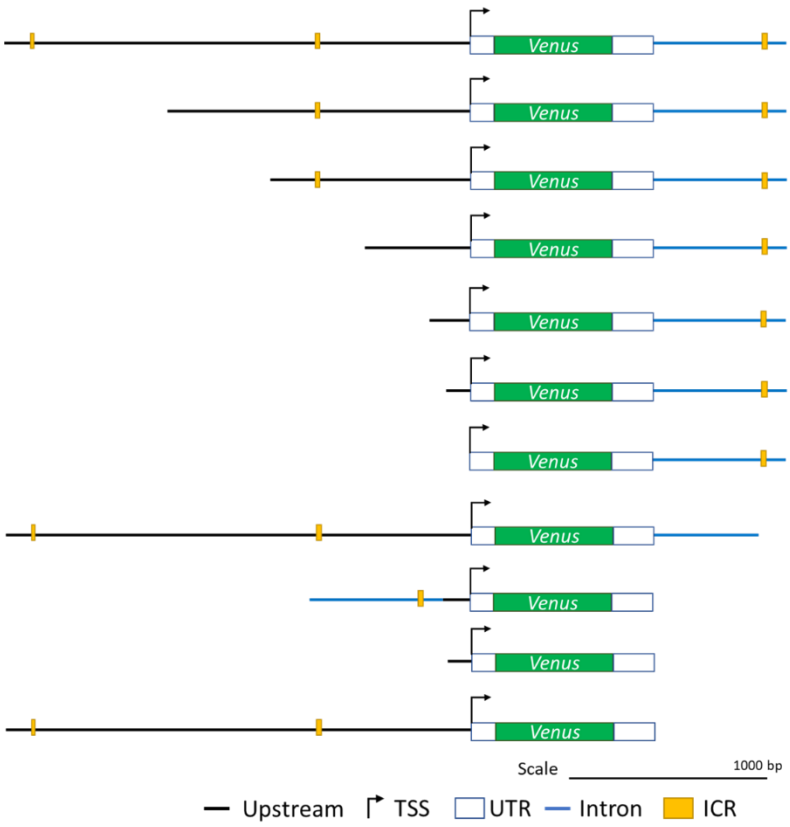

	n	Left Epidermis	A7.6	b-line
3000-Venus-Intron	32	78%	63%	78%
2065-Venus-Intron	19	84%	58%	68%
1379-Venus-Intron	27	63%	7%	63%
799-Venus-Intron	29	45%	17%	90%
395-Venus-Intron	12	33%	17%	75%
302-Venus-Intron	25	4%	0%	88%
146-Venus-Intron	24	0%	0%	13%
3000-Venus-ΔICR6	15	67%	40%	100%
Intron-395-Venus	8	0%	0%	13%
395-Venus	11	0%	18%	36%
3000-Venus	12	17%	25%	42%

Summary of the in situ hybridization results of deletion constructs with Venus probe. n: number of injected embryos. A7.6: trunk lateral cells derived from A7.6. b-line: epidermis on the dorsal midline and the secondary muscle at the tail tip, which are derived from b-line cells.

Supplementary Table S3 and 4 contain large data sets. So they can be downloaded at the following website.

http://www.bio.sci.osaka-u.ac.jp/bio_web/lab_page/nishida/shih/index.html

Supplementary Table S3. TFBSs predicted by the AnimalTFDB3.0 and filtered by the RNA-seq results in the Aniseed.
See Table S3.xlsx file.

Supplementary Table S4. Receptor proteins predicted by QIAGEN GENEGLOBE
See Table S4.xlsx file.